PERFORMANCE OF RC COLUMNS CONFINED WITH POLYUREA UNDER UNIAXIAL COMPRESSIVE CYCLIC LOADING

By

YASIR SIRAJ

(NUST-MCE-102292)

A dissertation submitted in partial fulfillment of the requirements for the degree of Master of Sciences in Structural Engineering

Supervised by

DR. MUHAMMAD RIZWAN

MILITARY COLLEGE OF ENGINEERING

NATIONAL UNIVERSITY OF SCIENCES AND TECHNOLOGY, RISALPUR

AUG, 2020

This is certified that following thesis

PERFORMANCE OF RC COLUMNS CONFINED WITH POLYUREA

UNDER UNIAXIAL COMPRESSIVE CYCLIC LOADING

Submitted by

YASIR SIRAJ

(NUST-MCE-102292)

Has been accepted for the completion of degree requirements for

MASTER OF SCIENCE

In

STRUCTURAL ENGINEERING

_____

Dr. Muhammad Rizwan

Military College of Engineering

National University of Sciences and Technology

Declaration

It is certified that the research work titled "***Performance of RC Columns Confined with Polyurea under Uniaxial Compressive Cyclic Loading****"* is my genuine work. This work has not been presented anywhere else for evaluation. The contents that have been obtained from other sources have been appropriately acknowledged and referred.

_____

YASIR SIRAJ

(NUST-MCE-102292)

Certificate for Language Accuracy

The thesis has been evaluated by an expert in English language and is certified to be free of typing, syntax, grammatical and spelling errors. The thesis is in line with the guidelines and format of university.

Student's Signature

_____

YASIR SIRAJ

(NUST-MCE-102292)

Supervisor's Signature

_____

Dr. Muhammad Rizwan

This work is dedicated to

My Family, Teachers and Friends

who give me the

courage and moral support

to accomplish this

significant event of my life.

Acknowledgements

All praises are for Allah, the Most Beneficent and the Most Merciful.

There are always ideas and persons behind a research that serve as a motivating force. These are the teachers, parents, friends, books, and research papers, experiences of the past and aims of the future. It is obligatory for me to extend my gratitude to all those aforementioned, with an explicit emphasis on a few.

I consider it my first and foremost obligation to express my heartfelt gratefulness towards ***Dr. Muhammad Rizwan*** for his guidance. He is really a knowledgeable and considerate supervisor. It is such an honor being one of his students.

I extend deepest respect and profound gratitude towards Dr. Hassan Farooq, Dr. Adeel Zafar, Dr. Tariq Feroze, Dr. Arshad Ali and Dr. Faisal Yousafzai for their encouragement and support throughout my work.

Words cannot express but my special thanks go to my family, especially my mother, whose unconditional love, prayers and uphill struggles throughout the life have been my greatest strength and a constant source of inspiration.

Last but not the least, I am thankful to my praiseworthy alma mater, MCE/ NUST, where I have been able to cultivate enough knowledge, strength and courage and build confidence in my abilities to explore the seemingly endless bounds of the knowledge.

Table of Contents

List of Figures

List of Tables

ABSTRACT

Reinforced Cement Concrete (RCC) has consistent use in construction industry worldwide. Due to the easy availability of its constituent materials, the flexibility of its forms, and the strength and economy it provides, RC structures are more preferred. The development of high strength concrete has improved rapidly due to industrial demand. But the increase in compressive strength of structural concrete introduces increased brittleness of concrete, and consequently, the brittle nature of high strength concrete is an obstacle in its extensive use. The performance of the RCC structure may not be enhanced merely by increasing its strength. The seismic performance of RCC structures entails that all the components of a structure, especially columns, should be able to dissipate large amount of energy while carrying the gravity loads. In this regard, member ductility, especially of column, is the key to performance of a structure against seismic effects. The confinement is one of the means to increase the ductility as well as compressive strength of concrete under compressive loads by restraining sideways expansion due to Poisson's effect. It assists a concrete segment to withstand plastic deformations without significant reduction in its strength. A significant amount of studies has been done in recent years to develop innovative confining techniques which could be applied to existing RCC structures, to improve their seismic performance. These confinement techniques are best option to make an existing structure, which is inadequate in seismic performance, safe against future probable earthquakes. The developed confinement techniques can also be affectively used in case of distresses caused by corrosion of reinforcement. However, each existing confinement technique has its inherit demerits, such as difficulty in application, cost, time and labor. Therefore, there is a need to introduce a new confining technique which can offset all or most of the indicated demerits. In this study, a new confinement technique, Polyurea is proposed that can be applied externally to existing

RCC structures, to enhance their seismic performance. The study presents a finite element method (FEM) based procedure to determine the effect on axial force and displacement capacity of RCC square columns due to confinement using Polyurea under axial compressive cyclic loading. The performance of rectangular RCC columns having concrete compressive strength of 4000 psi and 8000 psi, and provided with minimum reinforcement, confined with Polyurea is studied for uniaxial cyclic compressive load until failure. Confinement varies in thickness i.e. 2mm, 4mm and 6mm. The effectiveness of confinement is studied by comparing the results obtained from confined columns with control sample without confinement. Polyurea being a hyper elastic material and bearing a good deformability, significantly enhanced the yield, peak and ultimate force and displacement capacity, ductility index and energy dissipation of the RCC columns. The confinement effect of Polyurea is found very effective for RCC columns of normal and high strength concrete.

CHAPTER 1

INTRODUCTION

In this chapter, the overall introduction of the study is discussed. This chapter includes the background, problem statement, Objectives, Research Scope and Methodology of the research work is briefly explained.

1.1 Introduction

Reinforced Cement Concrete (RCC) also called reinforced concrete (RC) is consistently used in construction industry worldwide. Due to the easy availability of its fundamental materials, the flexibility in its forms, the strength and economy provided by it, RCC is usually preferred to other building materials.

Moreover, the use of high strength concrete has improved rapidly due to industrial demand because modern structures require increased strength and stiffness of structural members, which introduce additional advantages in the performance of structures. But the increase in compressive strength of structural concrete introduces increased brittleness of concrete, and therefore, the brittleness of high strength concrete is an obstacle in its prevalent use. The benefits in terms of reduced member size are therefore negated by the requirement for high factor of safety to avoid brittle failure i.e. risky and unacceptable.

Although strength is an obvious and basic factor in design of RCC structures but past and recent earthquakes have evidenced that during an earthquake, performance of RCC structure may not be enhanced merely by increasing its strength. It has been found that the capacity of structures to withstand large deformations in the inelastic range is also important to enhance its performance. The response of RCC structures to a seismic activity is highly dependent

upon the nonlinear material response of its members. Both the magnitude and cyclic nature of the displacements contribute significantly to the overall strength and stiffness of the structure.

In RCC buildings, the performance entails that all the components of a structure, especially columns, should be able to dissipate large amount of energy while carrying the gravity loads. In this regard, a member's ductility, especially of column, is the key to performance of a RCC structure against seismic effects. The confinement is one of the means to increase the ductility as well as compressive strength of concrete under compressive loads by restraining sideways expansion due to Poisson's effect (Ahmeda and Tahara 2015). It is an important factor for dissipation of energy because it ensures large plastic deformation to occur under greater loads. (Mander, et al. 1988) as shown in the figure 1. It allows a concrete member to withstand inelastic deformations without significant reduction in strength. Large deflections in a structure offer a good caution in the form of tensile cracks before a member completely fails; however, in any case the total collapse of the structure during an earthquake is not acceptable. In order to explore the behaviour of confined RC columns during an earthquake an analytical study is carried out in this project. This study presents a finite element method (FEM) based approach to investigate enhancement in the axial stress and strain capacity of RCC square columns due to confinement. The columns are provided with minimum steel reinforcement. Confinement is done using Polyurea and columns are loaded under axial compressive cyclic

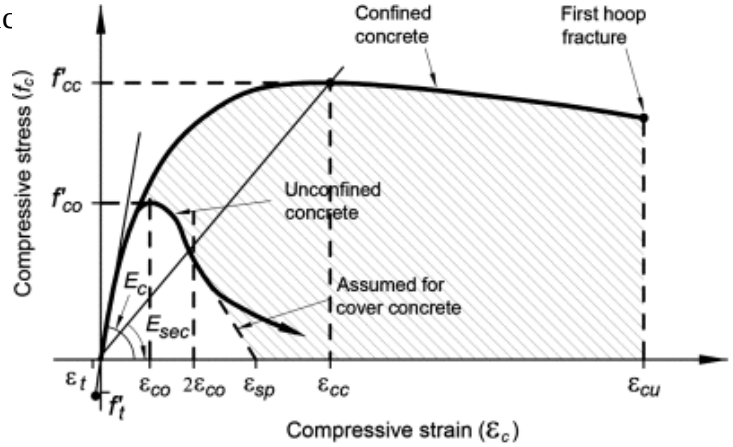

Figure 1. The Mander's model for confined concrete (Mander et al., 1988).

1.2 Background

This work is done on the basis of an experimental study conducted by A. E. Marawan, et al. 2015 in which the flexure and shear behavior of RC beams confined externally by sprayed Polyurea was studied. By studying different parameters including ultimate load, vertical deflection and overall ductility with effectiveness of variation of Polyurea thickness, it was found that:

1. The Polyurea provided greater ease of application and acted as containing material due to which the fragmentation was reduced.
2. The Polyurea coating system significantly increased the flexural and shear capacity of small and large scale beams.
3. The ductility of Polyurea coated samples was substantially greater than that of non-coated samples.
4. Polyurea enhanced the shear capacity comparatively more as compared to flexural capacity, which refers that the material can be used for effective confinement.

1.3 Problem Statement

Nowadays, viability of the built environment has turn out to be a major issue. Over the ages, new technologies have been developed and used for this purpose but any material or technology has its inherit demerits while coming across a new requirement of the modern era. A significant work has been done in past years to develop innovative rehabilitation and confining techniques to enhance the seismic performance of RC structures. Confinement is one of the best choices to make an existing inadequate structure safe for future probable earthquakes or other environmental forces. This technique decreases the liability of damage of a structure during an earthquake. Requirement for increase in compressive strength

concrete has introduced increased brittleness associated with it. I addition, corrosion of reinforcing steel in existing structures causes the concrete cover to spall off hence decreasing the gross area of a member for resistance to different types of stresses. Corrosion of reinforcement also reduces its effective cross-sectional area therefore causes degradation of its ultimate strength. Thus, it necessary to develop an innovative and optimum solution for retrofitting of members to remedy all the afore discussed problems at the same time.

Various confinement techniques have been developed to find out the state-of-the-art solution for these problems, yet a new hyper elastic material Polyurea can also be used for strengthening of such damaged structures. It is presumed that the Polyurea being a hyper elastic material bearing good deformability, axial, flexural and shear properties will enhance the ultimate strength, deformability, ductility and energy dissipation of the structures by resisting the secondary tensile stresses in transverse axis developed due to Poisson's effect. It may also be helpful in partial replacement of transverse reinforcement in the regions near supports where the volume of transverse reinforcement is relatively higher. In addition to the aforesaid advantages of Polyurea, it may be also helpful for the problem of strength degradation of reinforcing steel and spalling of concrete cover due to disruptive stresses caused by enlarged volume of corroded steel reinforcement as it bears good resistance for penetration of water.

1.4 Objective

To analytically study the performance of rectangular RC columns confined with Polyurea and compare it with the behavior of conventional tie reinforced RC columns in order to quantify the effectiveness of Polyurea in confinement.

1.5 Scope of Research

Performance of rectangular RCC columns having concrete compressive strength of 4000 psi and 8000 psi, confined with Polyurea and provided with minimum reinforcement of grade 60 in longitudinal axis and grade 40 in transverse axis will be studied for uniaxial cyclic compressive force until failure. Confinement will vary in thickness i.e. 2mm, 4mm and 6mm.

The following parameters will be used for comparison in this study.

1. Force-Displacement relationship.
2. Yield, peak and rupture load and displacement.
3. Energy dissipation.
4. Ductility.

A nonlinear analysis will be conducted using ANSY software, with isotropic elasticity and multilinear isotropic hardening properties of the concrete and steel materials used in the study, for the elastic range and post elastic (plastic) range including post peak region till failure and hyperelastic material parameters will be used for Polyurea.

1.6 Methodology

For analytical study of confined RC columns, constitutive models are selected from literature to define the material properties in ANSYS. Geometry, material properties and boundary conditions are defined for Finite element model. Two types of concretes are used to study the effect of ployurea on the response of normal as well as high strength concrete. The cross section of RC columns is designed according to ACI code. User defined outputs; longitudinal force and displacement are set as outputs for the finite element solution. Force-Displacement curve are drawn to study the overall response of confined RC columns. F-D curves are further used to study the confinement effect on peak and ultimate loads and displacements, ductility

index and energy dissipation in each loading cycle. The results of confined columns were compared with the unconfined one to investigate the effectiveness of Polyurea confinement in terms of the above said parameters. Flow chart of the methodology is given below.

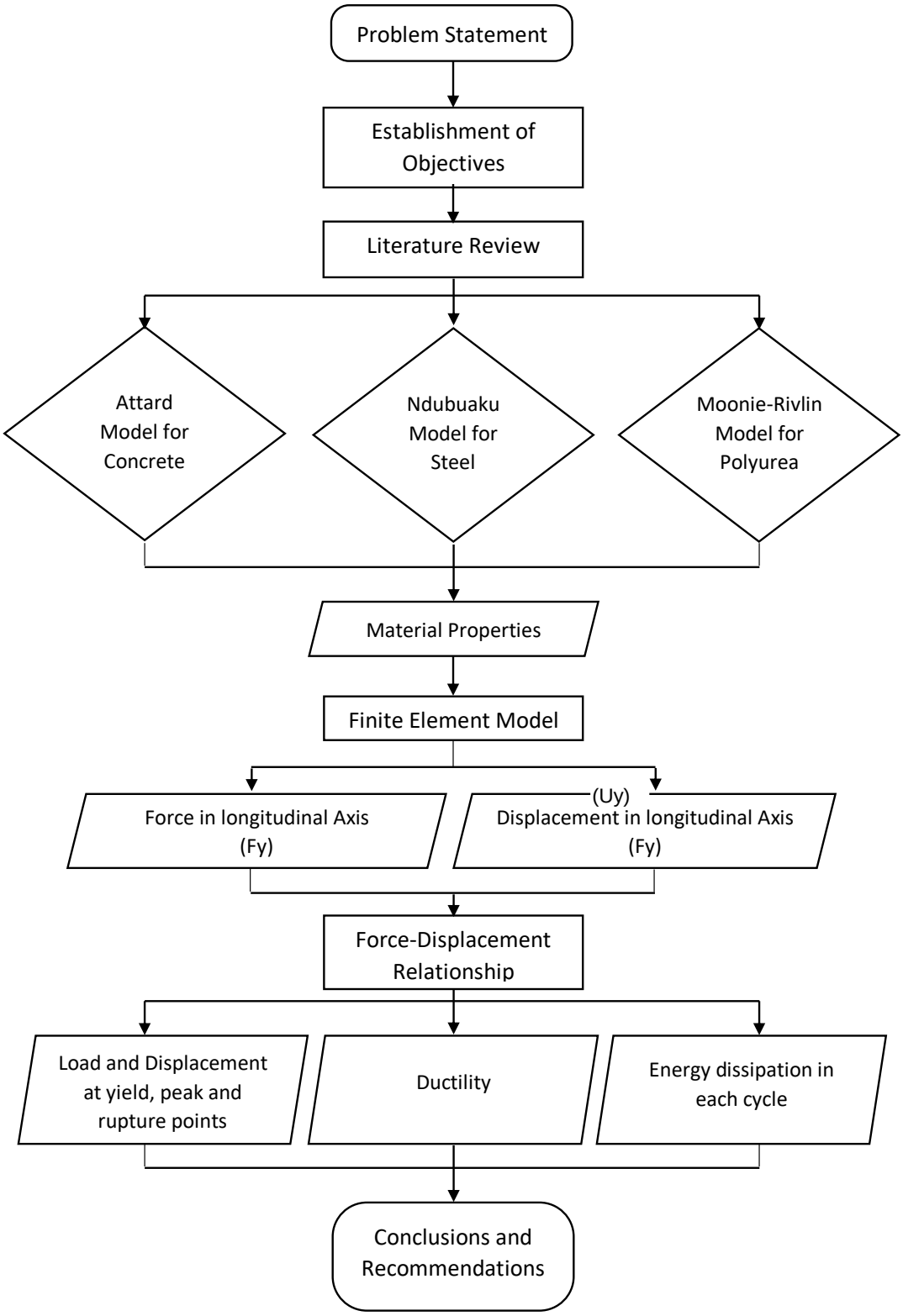

CHAPTER 2

LITERATURE REVIEW

In this chapter essential literature review for the study is briefly discussed. The concept of ductility is explained. Different existing techniques for active and passive confinement are explored and a detailed explanation of new/proposed confinement technique is discussed. General properties, advantages, application manner and literature about applications of Polyurea as a strengthening system in construction industry is also discussed in this section.

"Ductility is the Key to good (seismic) performance of Structures, Confinement is the Key for improving Ductility in Reinforced Concrete Members, and Moment-Curvature Relationship is the Key for computing Cross-Section and Member Ductility." (Mohiuddin Ali Khan, 2013)

The behavior of columns is the most critical aspect for the general seismic performance of a structure during an earthquake. The collapse of a column may lead to failure of whole structure or its major portion as it is the primary member for the stability of a structure. In most of the cases reported in earthquake destructions, the column plastic mechanism is normally found to be more frequent than the beam plastic mechanism. Most seismic design codes, such as ACI code's special provisions for seismic design, UBC and GB50011-2010 etc., entail that the columns must be stronger enough than the beams and other members to regulate the failure mechanism (Liu, et al. 2012) (YE, et al. 2010). It is a common fact that seismic performance of a structure subjected to cyclic load depends mainly on the compressive strength of its members but their ductility and ability for absorption and dissipation of energy is also an important factor (Rodrigues, et al. 2012). Ductility of concrete improves with confinement because it can sustain higher strains at peak load and it has a key role in the post peak branch of the stress-strain curve (Saatcioglbranch u and Razvi 1992).

2.1 Ductility

Ductility refers to the capability of a material, member or structure to withstand large deformation without failure. In place of elastic design of structures to resist lateral forces from severe and uncommon earthquakes, design of structures for lower force levels and higher ductility is more recognized practice in performance-based designs (Kristombu. Baduge, et al. 2019). Ductility is referred as the ratio of maximum deformation at the ultimate point to deformation at the yield point as shown in figure 2 and it is generally called as ductility ratio or ductility index, μ.

$$\mu = \Delta u/\Delta y$$

where Δu is maximum deformation and Δy is deformation at yield point.

Ductility describes the capability of structural members for deformations after yielding and dissipation of energy. In general, ductility is the property which defines the failure mechanism of a member. Worldwide, all seismic design codes accept the significance of ductility because it acts as a key in structural performance for seismic activities. The better the ductility, the larger the capacity of a structural element to experience plastic deformations without significant decrease in strength (Naveed and Fawad 2017).

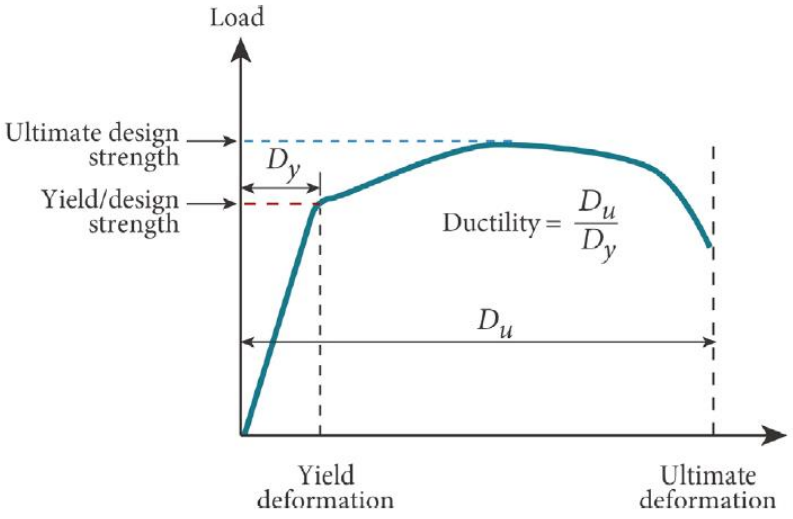

Figure 2. Definition of ductility ratio.

2.2 Confinement Techniques

The transverse confinement of a structural element is the most ideal choice to enhance the ductility of RCC members. There are two kinds of confinement procedures, active confinement and passive confinement. In active type of confinement, the member is pre tensioned before the application in a structural framework. During beginning of twentieth century, in about the entire of the directed researches, the compressive strength of RC was assessed by including the active confinement reaction of a proportionate liquid pressure. Passive confinement has been extensively utilized as a strengthening strategy to restore existing RCC buildings. Passive type of confinement requires a specific horizontal expansion of member before the activation of the confinement effect, while on account of active type of confinement, a pre-tensioned force to the enclosed material can eradicate with the necessities of such transverse enlargement (Chin, et al. 2018). In this section miscellaneous methods developed for confinement of RCC basic members are discussed.

2.2.1 Transverse Steel Reinforcement

In a frame structure it is necessary to ensure that columns are capable of behaving in a ductile manner. This is generally achieved by using transverse reinforcement as a confinement in the form of ties or spirals in the plastic regions as shown in the figure 3. At first time it was noted by (Ritchart, et al. 1928) that the concrete cylinders confined from the adjacent sides with steel plates presented excessive increase in the strength, stiffness, and strain at which the peak stress was achieved. This study resulted in the realization of effect of different parameters like shape, spacing and strength of confining and longitudinal reinforcement on performance of RC columns confined with this technique. Back bone curves of RC beam column joints confined with transverse reinforcement of steel stirrups is presented and comparison is made. The back bone curves of the cyclic response were used to determine

ultimate loads and ductility. During loading cycles, the response of the RC columns and their load capacity, ductility, residual displacement, degradation of stiffness and energy dissipation were compared. When considered different confining configuration and material strengths, assessment of the stress strain curves of confined concrete curves, indicated that they have important role in seismic response of RCC structures. When the concrete experienced deformation, there was a substantial increase in the capacity for loads and it failed progressively in a ductile way.

Some columns were tested by (Basset and Uzumeri 2011) under monotonic axial compressive force. The variables in the study were considered to be the tie configuration, their spacing and longitudinal steel distribution. From the results it was observed that the adding lateral confinement using steel remarkably enhanced the ductility of columns. The ductile behavior was found improving with increase in volume of transverse tie steel. The behavior is also found affected with the configuration of transverse reinforcement and well-distributed transverse steel resulted in improved behavior.

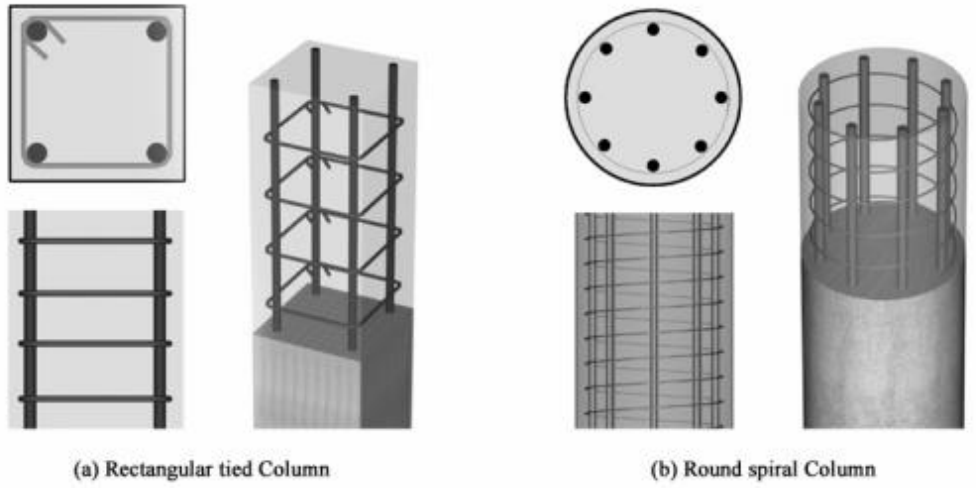

Figure 3. Concrete cylinders confined by transverse steel

2.2.2 Double Spiral Confinement

A batch of rectangular RC columns was cramped with a novel kind of dual spiral steel reinforcement. The columns were loaded for monotonic axial compressive force till failure. The double-spiral is a combination of two inter-connected spiral reinforcement that includes a round spiral at the middle and a star-shaped spiral nearby the boundary of the column as shown in figure 4.

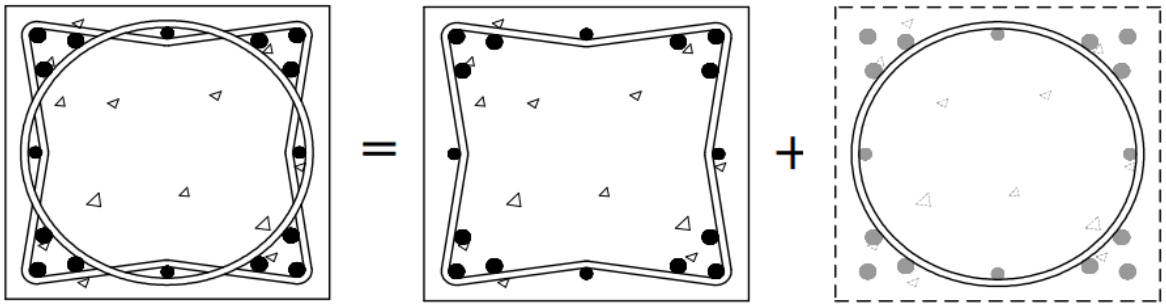

(a) Double-spiral (b) Star spiral (c) Circular spiral

Figure 4. The double-spiral confinement for rectangular RC column.

All columns were 600 mm square and 1200 mm in height. The major parameters of this study were the cost effectiveness, the efficiency of proposed confinement in axial strength and the ductility of the confined Double Spiral Reinforced Columns (DSRCs).

The ductility index, μ, was demarcated at the axial strain recorded at 70% of the post-peak load, to the strain measured at the peak load. From comparison of DSRCs to the RC column tied with conventional rectangular ties, it was discovered that, the ultimate strength of SRC columns was significantly higher than the traditional RC columns. Also, the ductility indices of the SRC columns, ranged from 3.03 to 3.99, which were much greater than that of 2.15 of the RC columns. This refers to that the proposed technique of confinement demonstrated excellent ability in strength as well as ductility. (C. C. Weng et al. 2008)

2.2.3 Expanded Metal Mesh (EMM)

This study presented a unique confinement technique that includes single expanded metal mesh (EMM) in addition to traditional transverse tie reinforcing steel as shown in figure 5. The EMM layer was wrapped above the tie bars. Sixteen square RC columns of 42.5 MPa C\compressive strength and slenderness ratios of 7.33 and 14 were provided with several volumetric proportions of tie bars. The columns were tested under uniaxial compressive force until failure. The parameters to be studied included ultimate force, axial deformations, ductility index, energy dissipation and crack production.

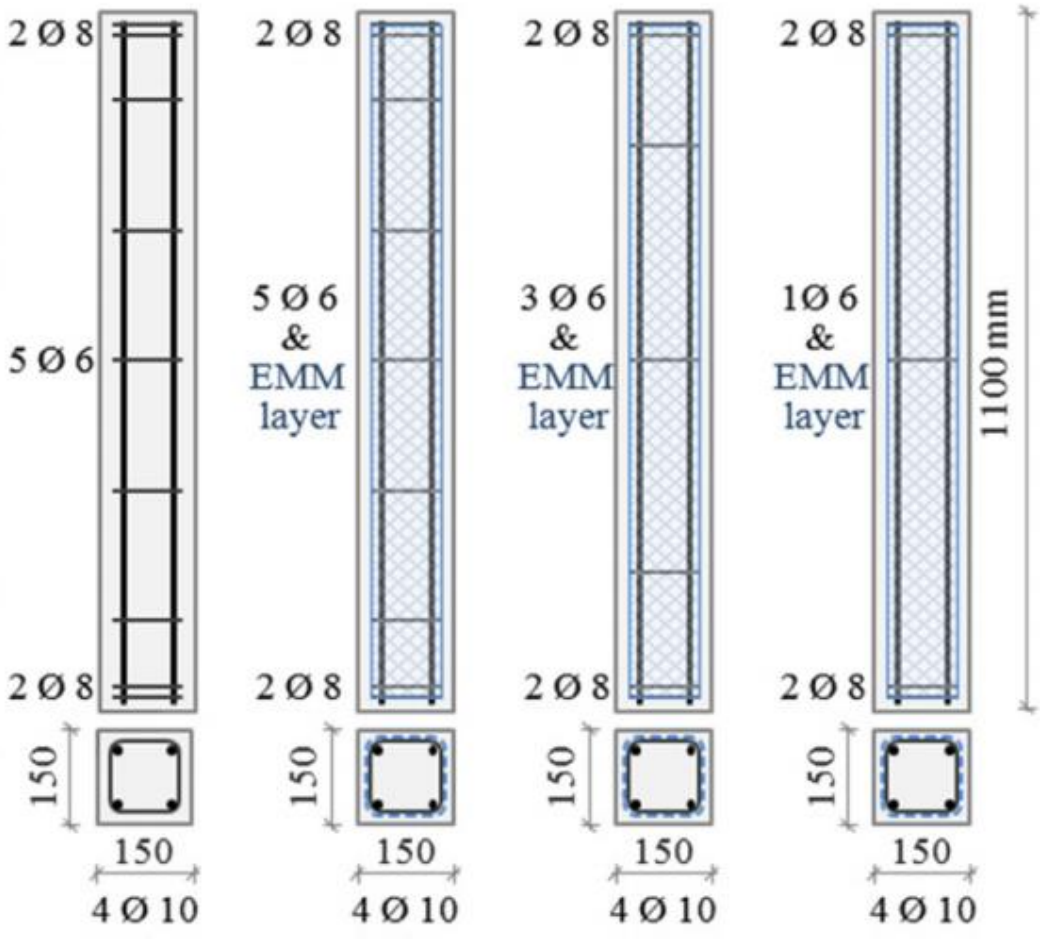

Figure 5. Details of columns wrapped with EMM

Based on the results conducted on 16 columns, it was concluded that RC columns confined with EMM layer in combination with tie bars experienced extra inelastic deformations and

more ductile response was observed, compared to samples confined with only conventional tie reinforcement. It was also observed that wrapping the columns with one EMM layer in addition to tie increased dissipation of energy 85.36% and 450.80% for samples with slenderness ratio 7.33 and 14, respectively. The ultimate load capacity was also increased by 11.02% and 18.55% for columns with slenderness ratios of 7.33 and 14, respectively. (Ahmed & Hany 2016)

2.2.4 Polypropylene Fiber Ropes (PPFR)

In this study high extension capacity PPFRs were used for external confinement for plain and reinforced square concrete columns having some corner radius. Polypropylene ropes were wrapped by hand in three and four layers and pretension force was applied to the PPFR ropes. Multiple series of increasing compressive deformations were applied on the columns and confined specimens were compared with the samples without pretension. From the results it was concluded that all the confined reinforced concrete columns offered improved stress–strain response with a more ductile post peak branch of the curve. The plastic modulus was highly improved. The effect of PPFR caused in the extension of the elastic response of the column by 40% in terms of load. Unwrapping of PPFRs after completion of test revealed that concrete core was cracked extensively and steel bars buckled. Pretensions of PPFR lead to an improved performance of the RC columns than PPFR wrapped without pre-stressing (Theodoros C. Rousakis 2014).

2.2.5 Thin Steel Plates

An experimental investigation was made for RC rectangular columns by changing the traditional lateral tie reinforcement by thin steel plates as shown in figure 6. Three square columns were casted with 150mm width and 910mm height, using various confining steel configurations. The concrete compressive strength was 18Mpa.

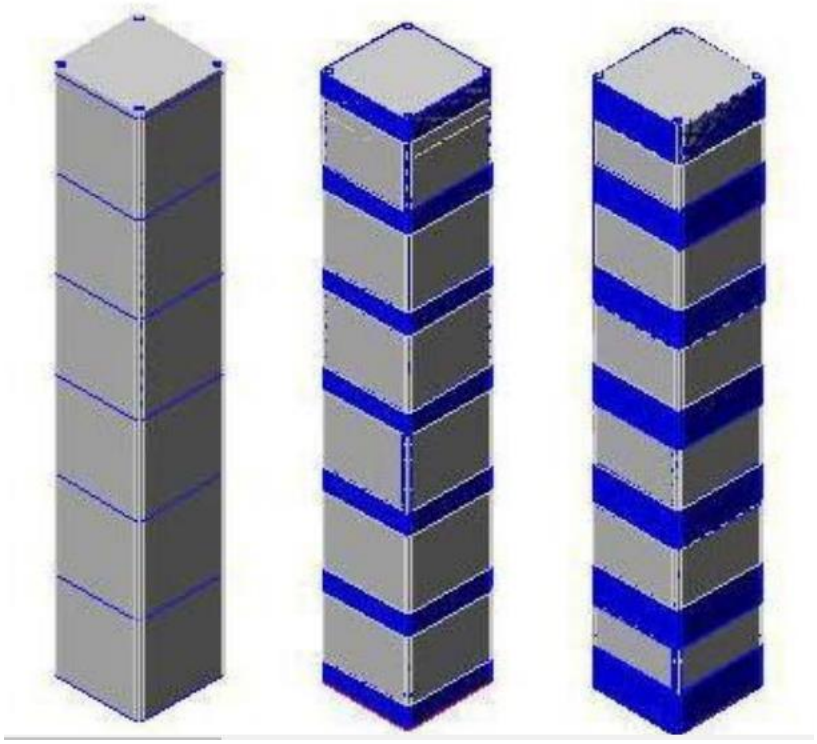

Figure 6. Details of RC columns confined with steel strips.

The parameters to be studied included maximum load capacity, the mode of failure and the ductility. There was a remarkable improvement in the strength and ductility for 2mm x 36 mm confining strip. Load capacity of the specimen confined with 2 mm steel strips was almost 78% higher than the control specimen and the specimen confined with 1.2 mm steel strips presented only 15.8 % larger capacity than the control sample (Ali A. and Shafqat A. 2012). The behavior of a concrete column confined by external steel rings was also investigated by (Safitri, et al. 2017). Two variables were studied which included the ring width and the distance between the rings. The coefficient of effectiveness of external confinement with steel rings was 0.89 which is very close to ideal value of 1.

2.2.6 Pre-Stressed Metal Straps

In this experimental study the concrete specimens were actively confined by using a strapping technique to enhance their overall performance. Normal strapping devices, that are normally used in the packing industry, were used in this study. The metal strips were pre

tensioned round the concrete columns. A batch of 72 cylindrical and prismatic concrete specimens was tested for axial compressive force. These samples were dynamically confined by metal strips and these strips were pre tensioned, thus increasing confining pressure. The influence of various parameters on ductility and ultimate stress and post peak behavior of confined concrete were studied. The variables included the compressive strength of concrete, volumetric ratio of confining strips, force applied to the strip and spacing of strips draped around the columns. The effect of confining metal strips on the performance of column specimens were investigated. From results it was evident that due to active confinement of metal strips, the ductility and strength of the specimen were significantly increased. It was noted that ductility of confining metal strips has an important role in improving the ductility of concrete. The increase in strength is primarily dependent on the effective volumetric ratio of confining straps. A stiffer elastic response of the specimen was observed as a result of active confinement by pre stressed metal straps as compared to the ordinary passive confinement (Moghaddam, et al. 2010)

2.2.7 External Steel Jacketing

In order to examine the influence steel jacketing on the performance of RCC columns, 7 RCC columns were tested having concrete compressive strength of 34 MPa. The size of the columns was 200mm x 200mm in cross section and 1200mm in height. The variables investigated in the study were in the shape of main strengthening system, number and size of confining steel plates. Details of jacketing system is shown in figure 8. On the basis of experimental results, it was concluded that external steel jacketing system for confinement RCC columns was very effective and it significantly increased the column's capacity for ultimate compressive load. The effectiveness of confinement increased when the effective area of the steel jackets enlarged. Also, the failure mechanism of columns was more ductile due to confinement by steel jackets strengthening system (Mahmoud, et al. 2015).

Figure 7. Details of steel jackets for confinement of columns

2.2.8 Fiber Reinforced Polymers (FRPs)

A large number of studies have been conducted to examine the effect of FRPs confinement on the performance of normal as well as high strength plain and reinforced concrete under compression and flexural forces. It is important to note that most of the experiments were carried out on RC column provided with small amount of transverse reinforcement. External confinement of concrete columns FRPs significantly enhances the strength, ductility and energy dissipation in hysteresis response. (Mirmiran and Shahawy 1997)

2.2.9 Carbon Fiber Reinforced Polymers (CFRPs)

The use of carbon fiber reinforced polymers is considered to be very effective confinement technique for reinforced concrete columns. Meanwhile the use of CFRPs materials is painstaking as it is more expensive than other strengthening methods, the cost of the material draws most of the attention.

A study was conducted using 17 reinforced and unreinforced concrete columns to investigate their performance due to external confinement using CFRP. RCC columns were strengthened with complete and fractional confinement to investigate their ultimate strength and ductility ratio increments. The performance of specimens was predicted with some parameters,

including failure response, ultimate load capacity, ductility index, and stress strain relationship. From experimental results, a significant increment in strength and ductility was observed for all of the complete and incomplete confined specimens. The completely confined plain concrete specimens, presented a substantial increment in ultimate load capacity and ductility ratio when compared to the control samples. However, the volumetric ratio of CFRPs were held same for all incompletely confined specimen and it was noted that the strength and ductility increment varies with the location of the jackets. The strength increase for RC columns was observed to be greater than for plain concrete columns. Moreover, the ultimate load capacity for completely confined reinforced concrete columns increased 100%, while for completely confined plain concrete columns the strength increased by 47% (C. S. Lewangamage, et al. 2017).

In another study, experiments were carried out on a batch of small scale 20 MPa circular plain concrete columns having 160 mm diameter and 320 mm height loaded for cyclic and monotonic loads that lead to a progressive buckling failure. The specimens were externally confined using CFRPs in various thickness and configuration shown in figure 7. From experimental results it was concluded that the effect of CFRP composites in confined concrete columns enhanced the ultimate load capacity with a considerable increase in ductility. Moreover, it was observed that CFRP used in the form of small width strips was the appropriate configuration for achieving optimum results (Riad and Abdelghani 2020).

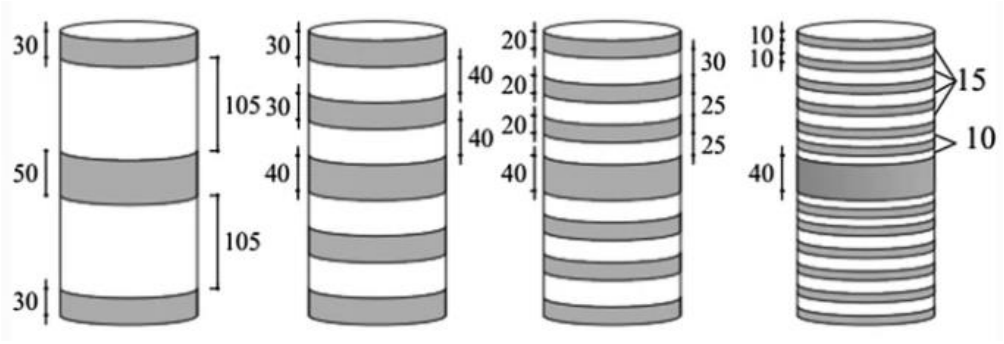

Figure 8. Detail of CFRP confined columns

2.3 Polyurea (PU): A new confining material

The continuing increase in necessities of the engineering structures is leading towards development and findings of up-to-the-minute, contemporary construction materials with outstanding parameters. Thin Spray on Liner (TSL) has been in popular use since the 1990s owing to their ease of application and minimal transportation of materials required. Recently, Polyurea (PU) a type of TSL has been receiving great interest from construction industry as structural reinforcement materials due to its tremendous advantages over conventional materials.

2.3.1 Introduction

Polyurea is made as an end result of mixing of 2 components i.e. isocyanate component and synthetic resin component. Reaction of these two components takes place in a high-temperature and high-pressure environments with suitable ratio of the aforementioned components. In the result of reaction, a chain-type structure is formed which contains "n" number of molecules that are strongly joint together (Fig. 9). This reaction takes place rapidly in a few seconds forming a hard hyper elastic material. The chain structure of the material makes it extremely durable and flexible and therefore it finds myriad of applications in construction industry (BASF). A comprehensive explanation of the development of Polyurea is described in (Grujicic, et al. 2012).

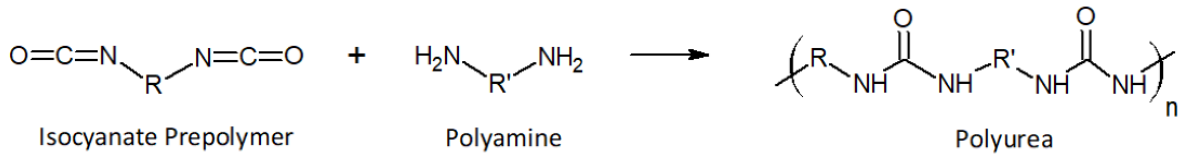

Figure 9. Chain structure of the Polyurea

The actual application of Polyurea was considered in ballistic devices and systems as it is highly capable of absorbing energy. It has apparently originated applications in construction industry, both in construction of new engineering projects as well as in renovation and maintenance of the existing ones. Polyurea is also used as a covering material for industrial floorings and as strengthening jacket for concrete (Szafran and Matusiak 2016). The reinforcing effect of PU appeared to be excellent under blast and impact as well as earthquakes. By using PU on concrete columns, the confinement effect can enhance their seismic strength and ductility (Cho, et al. 2017).

Figure 10. Photo of a typical Polyurea sample

2.3.2 Advantages of Polyurea

The primary benefit of the Polyurea coating is a rapid sheath preparation and application manner providing effective protection of a structural element. This technology can considerably decrease time to repair and the extent of work required for provision of external strengthening of components. (Szafran and Matusiak 2020)

Other advantages of the material include (Szafran and Matusiak 2016), (Maj and Ubysz 2017):

- Simplicity of application on top of any kind of surface.
- Great adhesion to most of the construction materials.
- Very high resistance for absorption and penetration of water.

- Highly resistant against confrontational atmospheric factors.
- Extraordinary resistance to mechanical damage.
- Great resistance to impulsive temperature fluctuations.
- Unimpeachable mechanical and durability properties.
- Hyper elasticity and flexibility of the material.

2.3.3 Application process

The application of Polyurea on a surface is a very complicated procedure. It basically comprises of three technical phases: (BASF)

1. Preparation of the surface onto which Polyurea to be applied.

2. Mixing of the reactive components in a high-temperature and high-pressure environment.

3. Application on the surface in the form of a spray with a specialized pump.

Surface preparation involves clearing of the surface from any contaminating particles with the use of either blast / sand-blast cleaning or the application of a priming paint to ensure firm adhesion. Since the application process requires special conditions of high temperature and pressure, a special plural-component sprayer is required for the process. The parameters of temperature, pressure and component proportions must be rigorously controlled as per the manufacturer's Product Data Sheet. Application is done in coats to ensure a fully leak proof surface and without welds. The number of passes and the speed of the passes determine the coating thickness.

2.3.4 Applications of Polyurea as a strengthening system

The actual application of Polyurea was considered in ballistic devices and systems as it is highly capable of absorbing energy. In recent years, elastomeric polymers found significance in retrofitting and strengthening techniques for structures actually exposed to explosions,

ballistic and impact loads. Recently, it has seemingly found applications in construction industry, both in construction of new engineering projects as well as in renovation and maintenance of the existing ones.

2.3.4.1 Blast resistance of RC panels

In this regard a study was conducted to present the outcomes from the experimental program and finite element analysis (FEA) to examine the performance of RCC panels coated with Polyurea and subjected to explosion effects. Three panels were tested (un-coated and Polyurea strengthened panels), and the FE analysis was done to simulate the explosion effects. The dimensions of the panels were 1700mm (L) × 1000mm (W) ×60mm (T). A panel was coated with 4 mm Polyurea on the surface opposite to explosion, whereas the second was covered with a 4 mm Polyurea coating on both surfaces and were subjected to explosion of one-kilogram Ammonite charge located at one-meter stand-off distance. Finite element model and analysis was done for the panels using the LS-DYNA's explicit solver. The outcomes from experimental and Finite Element Analysis recommended that though the Polyurea coating system improve the capacity of the RCC panels for absorbing the energy due to explosion, a greater level of safety is achieved form the protecting covering applied on the both surfaces of the panel. (Raman, et al. 2014)

2.3.4.2 Blast resistance of masonry walls

Three explosive experiments were conducted on Polyurea retrofitted masonry wall. All the tests included an explosion located away from a reinforced reaction structures containing masonry walls. The walls constructed in the reaction structure were around 2.24 x 3.66 m with a W 12x35 I shaped beam in between the two walls. The results of masonry wall tests markedly show that a Polyurea strengthening system for retrofitting of masonry wall against explosion was very functioning. The Polyurea coating effectively enhanced the resistance

against shock wave created by the explosive material. The control wall was collapsed and completely smashed while the Polyurea coated masonry wall persisted undamaged. No secondary disintegration was witnessed during the loading stage from walls strengthened on both of its sides. (J. S. Davidson, et al. 2004)

2.3.4.3 Bending and Shear resistance

A. E. Marawan, et al. 2015 investigated enhancement in the capacity of flexural and shear resistance of RC beams strengthened externaly by spraying Polyurea. They tested 16 samples of small scale and large scale RC beams made with a concrete having compressive strength of 25 MPa and reinforcement steel having yield strength of 400 MPa. The samples were coated with Polyurea having tensile strength of 12.98 MPa in thickness of 2mm, 4mm and 6mm. On the basis of results obtained from experiments, the authors concluded that the capacity of beams for flexural stresses increased by 11.2% in the case of large scale beams and by 19.4% in the case of small scale beams. The capacity for shear was increased by about 28% for large scale beams and by 42% for small ones. Polyurea represented more resistance for shear than flexure that refer to Polyurea may act as a confinement material as well. The Polyurea coating system showed more deflection during the failure of the beams which refer to enhanced ductility of the system. In general, Polyurea provided greater ease of application, make beams more ductile, and act as a containing material where fragmentation was reduced (A. E. Marawan, et el. 2015).

2.3.4.4 Crushing strength of RC concrete

In order to investigate the effectiveness of Polyurea coating system, nine concrete rings, made of class C25/30 concrete, was subject to a crushing strength test. Three components comprising the first batch were marked as control samples and were not Polyurea-coated. Three components of the second batch were coated with 2.5 mm thick Polyurea on their outer

surface. Three components of the third batch were coated with a membrane on their inner and outer surface. Concrete rings were 800 mm in diameter and 900 mm in height, and their shell was 100-mm thick. Structural reinforcement was provided in the form of three levels of perimeter rings made of a 4.0 mm rebar. Based on the results of experiments, a number of conclusions were drawn. The Polyurea coating system improved the crushing strength of concrete rings by 20.3% in the case of rings coated on both surfaces and it gave no effect in the case of rings coated on their outer surface. In the range of large strains, the Polyurea coating further increased the magnitude of destructive force. Moreover, concrete rings coated with Polyurea on both surfaces failed comparatively in a ductile way (Szafran and Matusiak 2020).

From literature, it can be observed that while this technique has been explored on various structural systems but its feasibility in concrete structures, especially as a confinement technique is yet to be investigated in detail, which is the subject matter of this study.

CHAPTER 3

CONSTITUTIVE MATERIAL MODELS

In this chapter the constitutive models used for different materials used for finite element model in the study are discussed. The constitutive model of Attard for concrete and used for 28 and 55 MPa concrete is explained. Engineering stress strain curve for steel and its conversion to true stress strain curve is also discussed. Constitutive models for steel are briefly discussed in this chapter. Mooney-Rivilin models for Polyurea are also discussed in the section. Mechanical properties of the material used for definition in ANSYS are discussed in this chapter.

3.1 Concrete

Determining the deformations of concrete subjected to any type of loading is a very complex thing to do. Due to inheriting heterogeneity of concrete, numerous factors affect the deformations. Among these factors a few can be mentioned here: the type of aggregate, the size and size distribution of the aggregate and the number and distribution of pores and voids. These are only some internal factors that can affect the deformations. Besides these, uncountable external factors may also influence the deformations of concrete. The complexity of concrete makes it very difficult to establish a correct constitutive model. The last some decades have seen a growing interest and use of high strength concrete and in many cases, they show a different behaviour than normal conventional concrete.

It is obvious that quite a lot of research has been done to describe the exact behaviour of normal and high-performance concrete deformations. In this section the unconfined concrete models for normal and high strength concrete will be discussed which will be used for

modeling and simulation of reinforced normal strength and high strength concrete columns in ANSYS for this study.

Analytical models for the full stress–strain relationship of confined and unconfined concrete in compression is the main requirement for the numerical simulation of the structural behavior of reinforced concrete structural elements. The first well-known study on the stress strain curve of concrete with and without confinement was done by (Richart, et. al 1928).

The earliest analytical models are attributed to (Hognestad 1951) who used a parabolic expression for the stress strain relationship. (Popovics 1973), (M. Sargin 1971), and (Ghosh, et al. 1971) proposed a mathematical fractional function for the stress strain relationship low strength concrete. (Kent and Park 1971) used a fractional equation for the ascending part of stress strain curve and a linear function for the descending part of the curve. Further improvements were developed by (Wang, et al. 1978). Others (Desaye and Krishnan 1989), (MacGregor 1992) have also worked for the development of unconfined and confined concrete models based on experimental and analytical studies. All These concrete models are either applicable only to a narrow band of concrete strengths or don't capture/ partially capture the complete response of the concrete accurately using finite element modeling and therefore, they are very difficult to calibrate to the specific concrete in question (Dahl and K.K.B 1992).

(Dahl and K.K.B 1992) worked on the relation between the uniaxial strength and deforamtional behavior of normal and high strength concrete by testing 7 different concrete mixes: 10, 35, 50, 70, 85, 100 and 110 MPa. They proposed a model based on the non linear elasticity of concrete which had an admissible similarity with the experimental results. They extended their work to include the poisson's effect and dilation of concrete, therfore, very smooth stress-strain curves were obtained. However, the proposed constitutive model relates very well to deforamational behavior of concrete but the following were the limitations.

1. The constitutive model covers only monotonically increasing compressive load.
2. This is only valid for short time loadings and the model doesnot include the effect of time on deformational response of concrete.
3. The model doesnot consider the tensile loadings nor the descending branch of the stress strain curve. For that reason it relied on the Ottosen linear model for descending region of the curve.

3.1.1 Attard Constitutive Model for Concrete.

A new analytical model for unconfined and confined concrete was introduced by (Attard and Samani 2012) which try to address the limitations in (Dahl and K.K.B 1992) model. Attard model is valid for a range of 20 MPa to 130 MPa. The proposed model is capable of predicting the non linear behavior of normal strength concrete, as well as high strength concrete in elastic, plastic and post peak regions of the stress-strain curve. The stress strain relationship in tension is assumed to be linear with a slope equal to elastic modulus in compression at zero stress. Comparison of Dahl model and Attard model is presented in Figure 11.

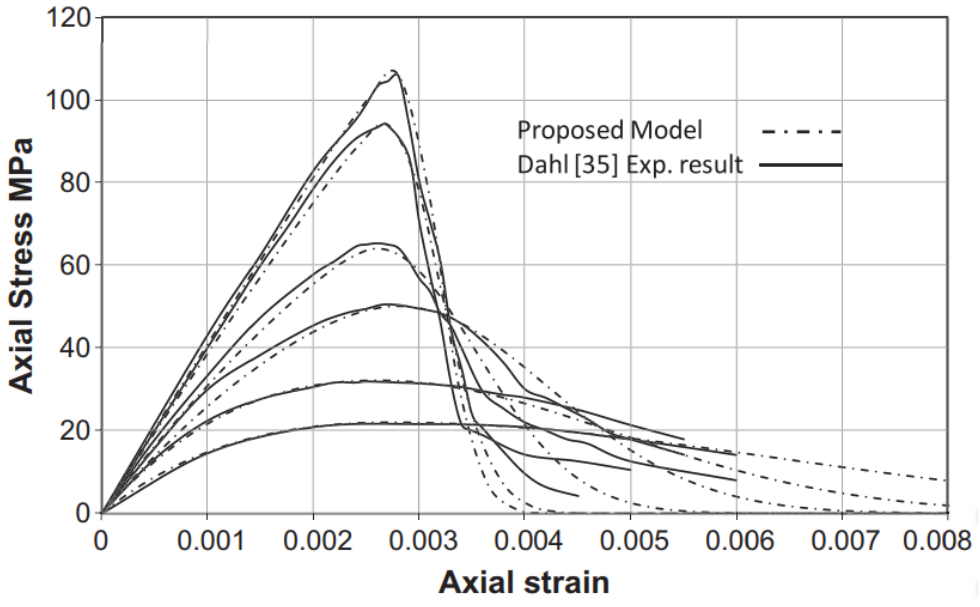

Figure 11. Comparison of Attard model and Dahl model

As the Attard new proposed model is shown to provide good predictions for the stress versus strain response for both uniaxial and triaxial compression, for normal strength and high strength concretes, for no to high levels of confinement and to take account of size effects due to varying specimen height and aspect ratio, therefore the data used for the calibration of this model is used for presentation of 28 MPa and 55 MPa concrete in this study as shown in figure 12. The stress strain relationship of 28 MPa and 55 MPa concrete reproduced from Attard used in this study is shown in figure 12.

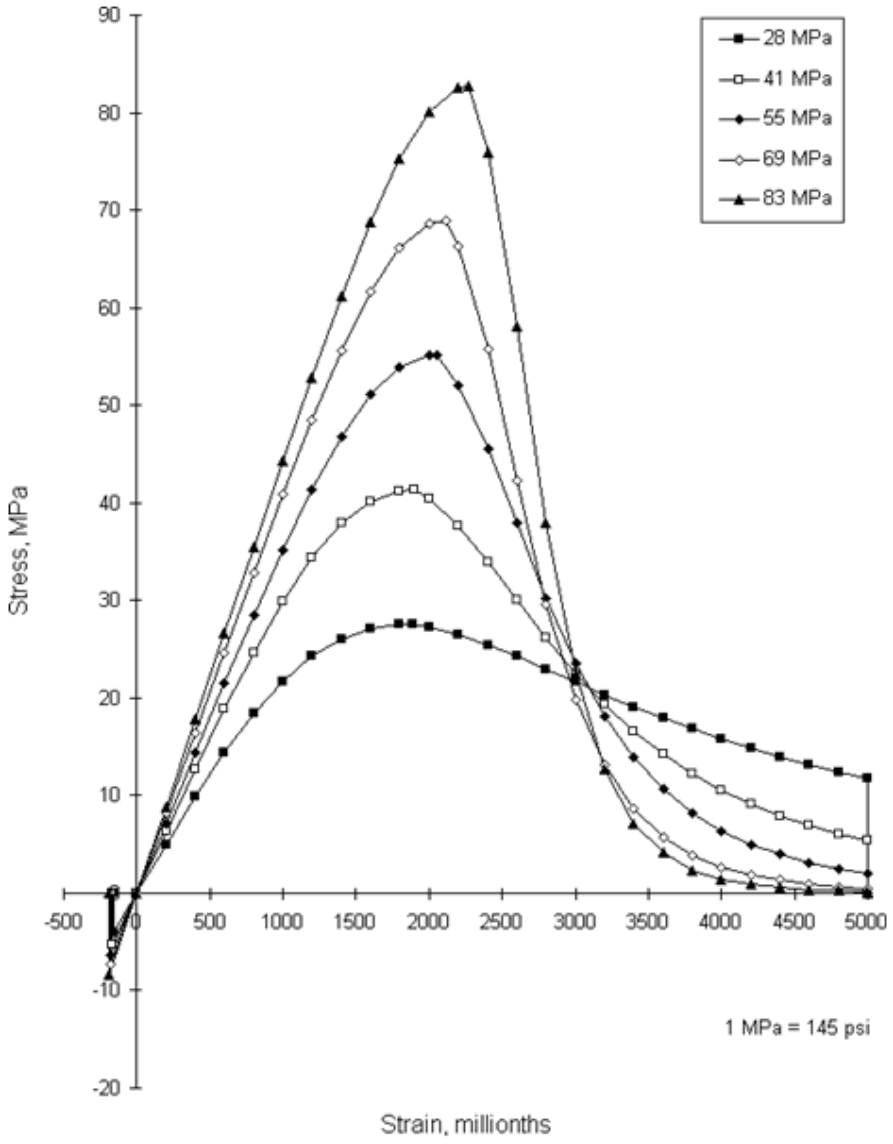

Figure 12. Stress-Strain relationship for concrete of different strengths (Attard).

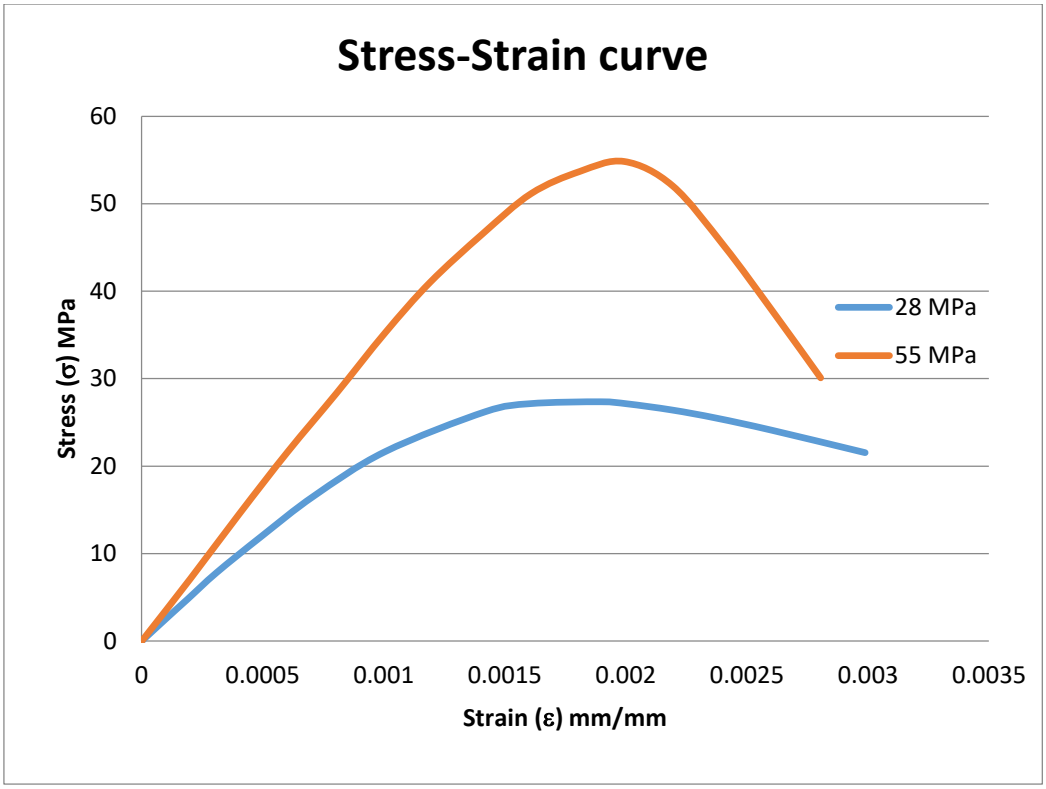

Figure 13. Stress-Strain curve for 28MPa and 55 Mpa

3.2 Structural Steel

The behavior of longitudinal as well as transverse steel may control the response of RC structural elements subjected to different loading. It is necessary to understand and define its fundamental characteristics that govern the actual behavior of steel within a range of loading that is applied on these structural systems.

3.2.1 Engineering Stress-Strain Curve

Steel is a ductile material and the stress-strain curve reveals many properties of the material under test such as elastic modulus, modulus of resilience, modulus of toughness, proportional limit, elastic limit, yield points, yield stress, ultimate stress, ductility etc.

Figure 14 shows a typical stress-strain curve for steel subjected to uniaxial tensile loading. Important characteristics of this response include:

Region I; Linear elastic region: Initial response is linear-elastic for stress demand less than the initial yield strength. In this region, when the loading is removed it returns to its initial position. Stresses are proportional to strains and it is referred as Hooke's law. The constant of proportionality in this region is modulus of elasticity or Young's modulus. The proportional limit stress is typically established by means of 0.01% strain offset method.

Region II; Non-Linear elastic region: In this region when the loading is removed it returns to its initial position but the stresses are no more proportional to strains. This region is referred as nonlinear elastic zone. The yield point Fy may be conveniently established as 0.2% strain offset method.

Region III; Yield Plateau: For strain demand exceeding that corresponding to the initial yield strength, there is a slight drop in strength below the initial yield strength. Strength is maintained at this lower yield strength for moderate increase in strain demand. This range of response is referred to as the yield plateau or the Lüders plateau, and the material yield strength typically is defined to be the average strength for loading within this strain range.

Region IV; Strain hardening region: Increasing strain demand results in increased strength. This strain-hardening regime is maintained to a peak strength that typically exceeds the yield strength by thirty to sixty percent. The ratio of peak strength to nominal strength is a function of the steel specification, grade and batch composition.

Region V; Strain softening region: At severe tensile strain demand, reinforcement begins to neck and strength is reduced. Once the specimen begins to neck, the distribution of stresses and strains become complex and the magnitude of such quantities become difficult to establish. At a maximum strain demand, the steel reinforcement fractures and load capacity is lost.

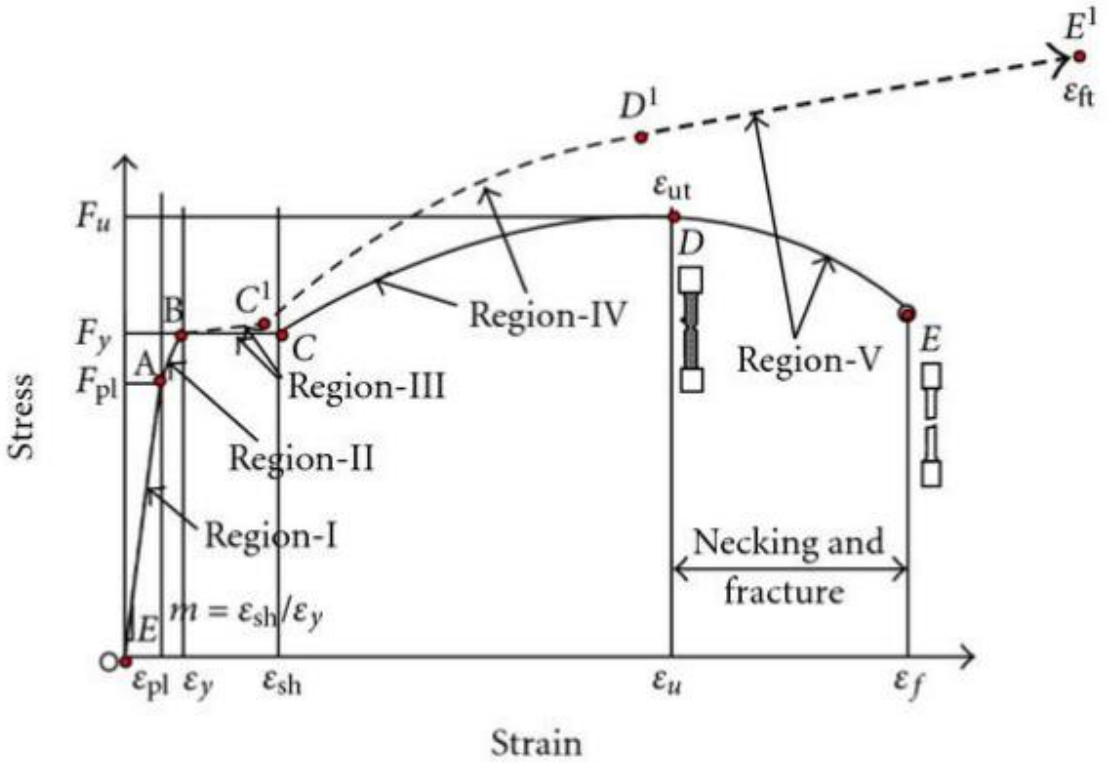

Figure 14. Typical stress-strain relationship of steel

3.2.2 True Stress-Strain Curve

For all practical purposes, the engineering relations and the true relations would coincide up to yield point; however, the two relations would diverge beyond this point.

Region I; Linear elastic region: The corresponding true stress and the true strain can be established directly from the engineering stress and the engineering strain based on the concept of uniform stress, small dimensional change, and incompressible material, which is valid for steel. Relations between engineering and true stress and strain are;

$$\sigma_t = \sigma_e (1 + \varepsilon_e) \text{ and } \varepsilon_t = \ln (1 + \varepsilon_e)$$

Where, σ_t and σ_e are the true stress and engineering stress and ε_t and ε_e are the true strain and the engineering strain, respectively. The difference between true stress and engineering stress at proportional limit stress may be about 0.2%; thus, the difference is insignificant in this region, therefore, the engineering stress and true stress are considered to be same.

Region II; Non-Linear elastic region: The true stress and true strain can be obtained in the same way as in the linear elastic range. Here, E_t is the tangent modulus given as

$$E_t = (\sigma_y - \sigma_{pl}) / (\varepsilon_y - \varepsilon_{pl})$$

Where the subscripts *y* and *pl* represent the yield and proportional points.

Region III; Yield Plateau: The engineering stress in this region can be assumed as a constant value of σy and the true stress and true strain can be obtained in the same way as in the linear elastic range.

Region IV; Strain hardening region: Though this region involves a nonlinear stress-strain relation, it is postulated that the true stress and the true strain can be obtained using the same relations as in linear elastic region. However, a power law is often used to relate the true stress to the true strain in this strain hardening region (Hollomon 1945) (M. Bruneau 1998). A power law of the form

$$\sigma_t = \sigma_{ut} (\sigma_u / \varepsilon_{ut})^n$$

Is used for the purpose, where σ_{ut} and ε_{ut} are the true stress and true strain associated with the ultimate tensile strength σ_u. The value for n must be established for different steel grades which may be achieved using a least square analysis of the corresponding experimental results.

Region V; Strain softening region: The apparent stress strain curve in this region is due to the use of the original cross-sectional area, and when the actual cross-sectional area be used, the stress and strain would continue to increase. The true stress-strain relations cannot be established in this region simply from engineering stress-strain values; thus, an experimental-numerical iterative approach was developed by (Zhano and Li 1994) to derive the true

stress-strain material characterization for this region. They proposed that the parameters for a true stress-true strain relation be determined by using iterative FE method with an experimental tensile load-extension curve as a target. Although this method establishes the true stress-true strain relations from standard tensile test results without measurements of the deformed dimensions of the test specimens, therefore, the main shortcoming is that the entire stress-strain relation during necking is treated as an unknown and a trial and error procedure is used for a series of strain intervals until good correlation with the experimental results is attained. By nature, this method is computationally intensive and time consuming.

(Ling 1996) proposed a weighted-average method for determining the uniaxial true stress versus true strain relation during necking. According to him, a power-law fit, which represents strain hardening region of the flow curve, can be used as the lower bound whereas a linear strain hardening model can be used as the upper bound. The upper bound linear hardening model could be

$$\sigma_t = (a_0 + a_1 \varepsilon_t),$$

Where constants $a_0 = \sigma_{ut}\,(1 - \varepsilon_{ut})$ and $a_1 = \sigma_{ut}$.

3.2.3 Model for True Stress-Strain Curve of Steel

Characteristics of reinforcing steel are generally established through laboratory testing of steel samples, however, on the basis of experimental results, many researchers have provided different theories and techniques for establishing analytical models that truly predicts steel response under loading.

The true stress-true strain characterization of a ductile material such as steel may be established using a constitutive mathematical expression such as the Ramberg-Osgood

equation or others. The Ramberg-Osgood stress strain equation, which expresses the strain as a function of the stress and is governed by two material constants (the 0.2% proof stress $\sigma 0.2$ and the initial elastic modulus Eo) and one model constant (the strain-hardening exponent, n), has been widely-adopted for many civil engineering applications but has also been observed to be incapable of providing excellent approximations of material stress-strain behavior beyond the 0.2% proof stress (P. Arasaratnam 2011).

In a bid to improve the predictive accuracy of the Ramberg Osgood equation, a number of modified stress-strain expressions have been subsequently put forward by several researchers. Most of the modified expressions are however designed to capture the tensile stress-strain behavior of metallic materials at room temperature. (Ramberg and Osgood 1943, Skelton et al. 1997, Macdonald et al. 2000, Mirambell and Real 2000, Chryssanthopoulos and Low 2001, Gardner and Nethercot, 2004). However, there are some important limitations associated with existing stress-strain models: some models lack the desired robustness and accuracy for defining a wide range of stress-strain behaviors, and the applicability other models is hampered by the large number of constituent parameters required for improved accuracy. (Ndubuaku Onyekachi 2017)

A novel stress-strain model providing an accurate approximation of the stress-strain behavior of metallic materials at different temperatures and strain rates was presented by (Ndubuaku Onyekachi 2017). The practicality and efficiency of the proposed model was illustrated by comparison of model-approximated stress-strain curves (derived using the proposed equation) to experimental stress-strain curves and over a wide range of temperatures and strain rates, excellent correlations were observed for all the comparisons.

As the (Ndubuaku Onyekachi 2017) model addresses many limitations and complications of the previously developed models, therefore, the data from this model was reproduced for

modeling a 280 MPa and 420 MPa steel in this study. Stress strain curve for 280 MPa and 420 MPa steel is shown in figure 15.

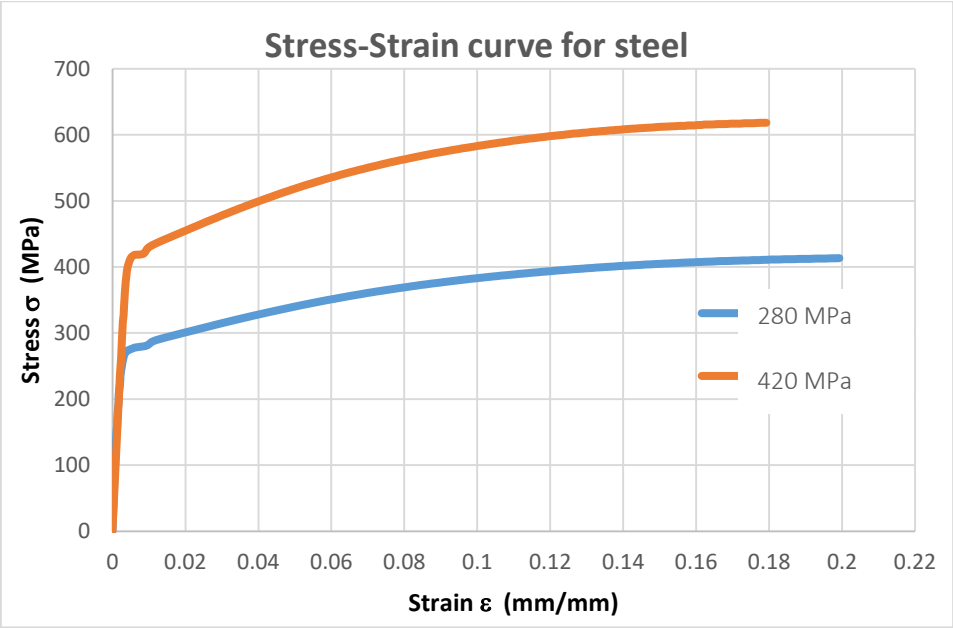

Figure 15. Stress-Strain curve for steel

3.3 Polyurea

The relevant literature reveals that a number of mechanical experiments have been performed to characterize the mechanical response of Polyurea at low and high strain rates. These experiments have demonstrated that the Polyurea shows highly elastic and almost incompressible behavior. Although, the experimental response of Polyurea has been described for a broad range of strain rates but the exact material modeling for finite element analysis is still a scarce.

(Yi J., et al. 2006) in their research, investigated the behaviour of one Polyurea sample and three polyurethane ones under compression force. They work was done using a Hopkinson pressure bar system. An analysis of the results unveiled a visibly nonlinear, stress-strain relationship which greatly depended on the strain rate.

(Sarva SS, et al. 2007) worked on the behaviour of a sample of Polyurea for a relatively broad strain rate range: from 10^{-3} to 10^{4} s^{-1}. Based on the results of the performed experiments, it was seen that the stress-strain relation for Polyurea changes its features from rubber-like material at low strains to leather-like at high strains. Its characteristics are determined by the structure of the mix. The ultimate product is hiper elastic and practically incompressible. It may be made softer at ultra-high temperatures (Szafran and Matusiak 2020).

(Amirkhizi, et al. 2006) proposed a viscoelastic constitutive model for Polyurea which includes time–temperature superposition and linear pressure sensitivity. The model was revealed to forecast the high strain rate behavior of Polyurea in tension with rational precision. The work of (Li and Lua 2009) is established on the basis of Ogden model and Zapas kernel model to achieve the hyper-elastic and visco-elastic performance of Polyurea. This model was revealed to fit with the compressive loads only.

The selection of model is mainly dependent on its purpose or application, basic variables involved and the data available to define the material properties. More or less, the existing hyperelastic models for finite element analysis are: Neo-Hookean, good to work in a strain range 30%, Mooney-Rivlin up to 30% in compression and 200% in tension, Arruda-Boyce for 300% and Ogden for high strain rates up to 700% (Kumar and Rao 2016).

Although the aforementioned models are comparatively successful in replicating the experimental data, they are not so straightforward to implement for engineering practice and have only been shown to fit with one type of loading test, i.e. either in compressive or tensile loading model (Kumar and Rao 2016).

The Moonie Rivlin (MR) constitutive model has presented potential for correctly present the nonlinear σ-ε response of most isotropic hyperelastic materials like polymers, silicon, rubber,

and Polyurea, besides this model is strain rate independent. Therefore, it has been widely used in many researches and finite element analysis as a constitutive model to represent the behaviour of hyperelastic materials. The MR model with 9 parameters is widely used in finite element analysis for hyperelastic materials (D. Mohotti, et al. 2014). And therefore, the MR 9-parameter model is used in this study to represent the behaviour of Polyurea. The material constants found by (C.Gamonpilas 2012) were used to model Polyurea with MR 9-parameter model in this study. Material constants are given in Table 1. The density of material is 1.0g/cm^3 and ultimate tensile strength was 19.2 MPa. Other mechanical properties found by the authors are given in the Table 2.

3.3.1 Moonie Rivlin 9-Parameter Model

MR model is a distinct form of Polynomial model. When N = 1, the Polynomial model is condensed to 2-parameter MR model, when N = 2, the Polynomial model is set to 5-parameter MR model and when N = 3, the Polynomial model is presented as 9-parameter MR model (WELSIM 2013). The general forms of MR models are given below where "*c"* represent empirically determined material constants and "*D"* is incompressibility parameter.

Two parameter Mooney Rivlin model:

$$W = c_{10}\left(\bar{I}_1 - 3\right) + c_{01}\left(\bar{I}_2 - 3\right) + \frac{1}{D_1}(J-1)^2$$

Three parameter Mooney Rivlin model:

$$W = c_{10}\left(\bar{I}_1 - 3\right) + c_{01}\left(\bar{I}_2 - 3\right) + c_{11}\left(\bar{I}_1 - 3\right)\left(\bar{I}_2 - 3\right) + \frac{1}{D_1}(J-1)^2$$

Five parameter Mooney Rivlin model:

$$\begin{aligned} W &= c_{10}\left(\bar{I}_1 - 3\right) + c_{01}\left(\bar{I}_2 - 3\right) + c_{20}\left(\bar{I}_1 - 3\right)^2 \\ &+ c_{11}\left(\bar{I}_1 - 3\right)\left(\bar{I}_2 - 3\right) + c_{02}\left(\bar{I}_2 - 3\right)^2 + \tfrac{1}{D_1}(J-1)^2 \end{aligned}$$

Nine parameter Mooney Rivlin model:

$$
\begin{aligned}
W &= c_{10}\left(\bar{I}_1-3\right)+c_{01}\left(\bar{I}_2-3\right)+c_{20}\left(\bar{I}_1-3\right)^2 \\
&+ c_{11}\left(\bar{I}_1-3\right)\left(\bar{I}_2-3\right)+c_{02}\left(\bar{I}_2-3\right)^2+c_{30}\left(\bar{I}_1-3\right)^3 \\
&+ c_{21}\left(\bar{I}_1-3\right)^2\left(\bar{I}_2-3\right)+c_{12}\left(\bar{I}_1-3\right)\left(\bar{I}_2-3\right)^2+c_{03}\left(\bar{I}_2-3\right)^3+\frac{1}{D_1}(J-1)^2
\end{aligned}
$$

Table 1. Material constants of Polyurea for MR 9-Parameter model in MPa.

C_{10}	C_{01}	C_{11}	C_{20}	C_{02}	C_{21}	C_{12}	C_{30}	C_{03}	D_1
12.369	8.124	-17.653	7.274	3.062	-0.437	-0.298	0.043	2.94	0

Table 2. Mechanical properties of Polyurea.

Mat Type	Density (g/cm^3)	E Modulus (MPa)	Shore D Hardness	Elongation (%)	Bending Strength (MPa)	Tear Strength (MPa)	Tensile Strength (MPa)
XS-350	1.0	100	60	162	18.1	13.7	19.2

CHAPTER 4

FINITE ELEMENT ANALYSIS

In this chapter the concept and steps involved in Finite Element Analysis is discussed in this chapter. First of all, introduction to finite element analysis is given. Then, literature about finite element analysis done by different researches is discussed. In the end the finite element model used in this study and the steps involved in finite element analysis are explained with reference to this study.

4.1 Introduction to Finite Element Analysis

According to (Bathe 2014), it is quite difficult to assess an exact date of discovery, as is often the case for original inventions, but the origins of the finite element method can be traced back to three different groups; applied mathematicians (Courant 1943), doctors (Synge 1952), and engineers (Argyris 1954). Although in code published already, the finite element method got its real motivation from the developments of engineers. The original contributions appeared in the papers by (Argyris 1954), (M. J. Turner 1956), (A. Kelsey 1960), (Zienkiewicz 1964) and (R. W. Clough 1968). The name finite element was first time coined in the paper by (R. W. Clough 1968). Significant contributions in the earliest were those of (Argyris 1954) and (Zienkiewicz 1964). Since the early 1960s, a number of researches has been dedicated to this technique, and a number of publications on the finite element analysis is presented. Initially, the finite element method in engineering was developed for the analysis of structural mechanics' problems on a physical basis. It was soon recognized, however, that the technique could be applied equally well to solving many other kinds of problems.

Some of the relevant research works are compiled in the following section about the finite element modeling of reinforced concrete members. Which are split in two main categories: confine concrete columns and all other concrete members are listed under the different category.

4.2 Finite Element Analysis of RCC Columns

This section of the chapter includes the previous research on reinforced concrete columns tested experimentally and modeled in finite element modeling software's for the simulation of the specific columns.

1. (Minafò 2019) investigated the effect of steel jackets in confinement of concrete and suggested an analytical model which is based on experimental data from the literature. The authors selected different parameters to identify the most significant parameters that affect the overall performance of externally confined concrete under axial load. The model was validated through a finite element analysis module; ATENA and compared with experimental data. The authors concluded that the proposed analytical model was reliable.

2. (Campione, et al. 2017) studied the behavior of RCC column confined externally through angles and battens. The authors focused on two parameters of the new confining technique: the friction effect of the angle with concrete and the cohesion effect between angle and concrete. They modeled the column in finite element module; OPENSEES and checked the effect of both parameters. The authors proposed a new model which included the effect of cohesion and friction. The proposed model was then calibrated and validated in OPENSEES.

3. (Rizwan, et al. 2016) studied the experimental hysteresis response of steel-strip confined reinforced concrete column and the data obtained was calibrated in finite element software; DRAIN-3DX. From the calibration the author presented the models for concrete and steel.

The authors also studied the behavior of the 8-story building using the calibrated models of the materials.

4. (T. Yu 2010) experimentally studied rectangular and circular columns with different arrangement of confining reinforcement and presented a modified plastic-damage model within the theoretical framework of the Concrete Damaged Plasticity Model (CDPM) in ABAQUS for the modeling of confined concrete under non-uniform confinement. The modifications proposed for the CDPM included a damage parameter, a strain-hardening/softening rule and a flow rule, all of which are confinement-dependent, and a pressure dependent yield criterion.

5. (Han, et al. 2009) investigated the performance of high strength concrete columns confined through aramid fiber reinforce polymer jackets. From the experimental data they developed an analytical model for predicting the stress strain curves and using a finite element software; ANSYS. They validated the analytical model against the experimental result and obtained promising results.

6. (Doran, et al. 2009) studied the nonlinear response of rectangular and square columns confined with fiber reinforce polymers. The authors used the literature data for finite element modeling using LUSAS and checked that data in term of axial strain to lateral strain. On the basis of results, they concluded that the stress-strain behavior of confined concrete was in close agreement. The authors suggested that to comprehend accurately the behavior of FRP confined rectangular column there is need of more analytical and experimental work.

7. (Tavio, et al. 2009) studied the nonlinear performance of confined reinforced concrete columns under axial load using finite element software; ANSYS. They studied four columns with different configuration of transverse reinforcement. The investigators concluded that ANSYS is capable of modeling reinforced concrete columns.

4.3 Finite Element Model: ANSYS

In this section the finite element procedure for this study will be discussed. Although structural modeling using numerical methods are applied in FEM solutions for many years, we cannot forget the sense and the procedures involved when a FEM procedure is ongoing. The common FEM procedure is well explained by (Bathe 2014). A mathematical model including differential equations describing the geometry, the kinematics, the material law, loadings and boundary conditions, and other elements, describes the investigated physical problem. The FEM solution passes through the identification of finite element types, the mesh density, and the solution parameters. Finally, an assessment of the accuracy of the FEM solution is investigated, and eventually, the mesh is refined, along with some changes to the model. In the final phase, the results are interpreted, and the analysis could be redone for detailed refinement or for the improvement due to the structure of the final optimization. One of the implicit limits of the FEM procedure is that it represents only a simplified description of a physical model, as the most refined mathematical model is not able to reproduce all the information that is present in nature. FE models are mathematical models and can represent physical problems only if they are accurately described. For this reason, a FE model must be obviously checked for its reliability with an accurate final assessment.

4.3.1 Geometry

The geometry of the RC column confined with Polyurea has been designed in SpaceClaim, a drafting software and further refined in ANSYS DesignModeler, an environment which is used to generate a parametric geometry for analysis. ANSYS DesignModeler provides unique modeling functions for simulation that include parametric geometry creation, concept model creation, CAD geometry modification, automated cleanup and repair, and several custom tools designed for fluid flow, structural and other types of analyses. The cross

section of the RC column is 152.4mm x 152.4mm and the height is 1000mm as shown in figure 16. External confinement is provided in various thickness; 2mm, 4mm and 8mm. 4 #4 longitudinal bars and #3 transverse bars with 305mm c/c spacing are provided with 20mm concrete cover. The detailed geometry of the RC column confined with 2mm Polyurea in SpaceClaim and DesignModeler are shown in figure a and b other samples are similar to this one.

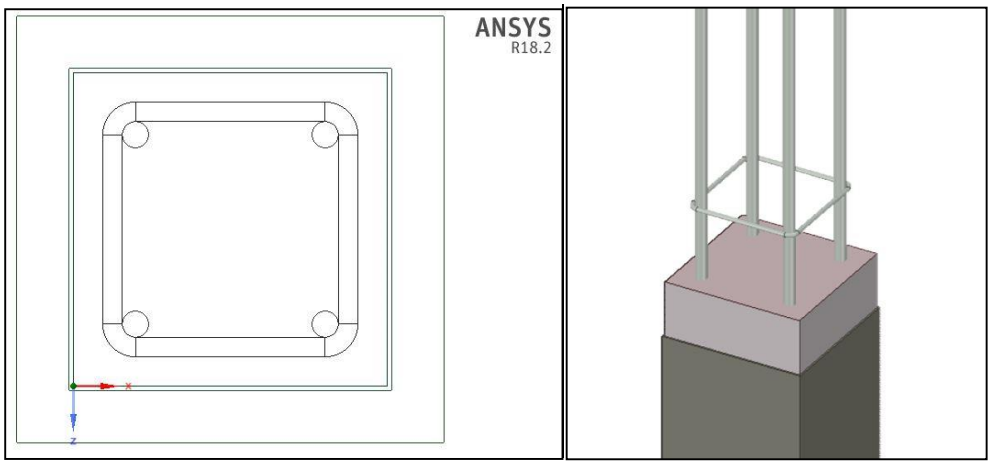

Figure 16. Cross section of RC column with confinement

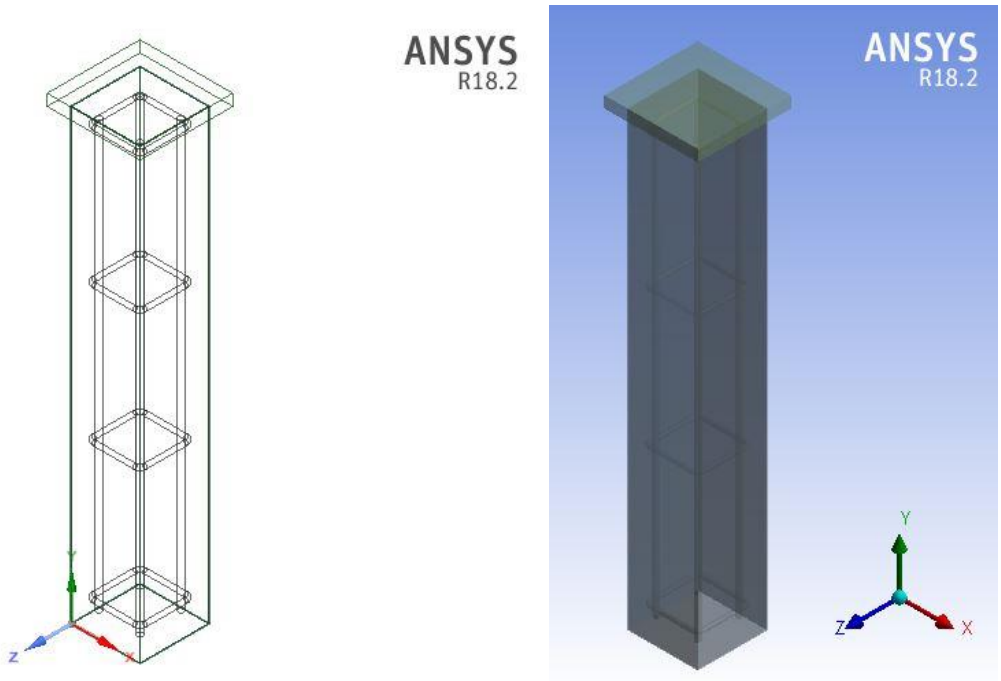

Figure 17(a). SpaceClaim Geometery *Figure 17(b). DesignModeler Geometery*

Figure 17.(a) and (b) Geometry of RC column with confinement

Model (A4) > Geometry > Part 2 > Parts

Object Name	*Tie\Solid*	*Tie\Solid*	*Tie\Solid*	*Tie\Solid*	*4K2MM\Rebar1*	*4K2MM\Rebar2*	*4K2MM\Rebar3*	*4K2MM\Rebar4*	*4K2MM\Concrete*	*4K2MM\Polyurea*
State	Meshed									
Graphics Properties										
Visible	Yes									
Transparency	1									
Definition										
Suppressed	No									
Stiffness Behavior	Flexible									
Coordinate System	Default Coordinate System									
Reference Temperature	By Environment									
Behavior	None									
Material										
Assignment	Structural Steel G40				Structural Steel G60				Concrete 4k	Poly Urea (Mooney-Rivlin Model)
Nonlinear Effects	Yes									
Thermal Strain Effects	Yes									
Bounding Box										
Length X	123.83 mm				12.7 mm				152.4 mm	156.4 mm
Length Y	9.525 mm				952.14 mm				1000. mm	
Length Z	123.83 mm				12.7 mm				152.4 mm	156.4 mm
Properties										
Volume	31219 mm³				1.2061e+005 mm³				2.2618e+007 mm³	1.2352e+006 mm³
Mass	0.24507 kg				0.94682 kg				49.761 kg	1.2352 kg
Centroid X	76.198 mm				30.163 mm	122.24 mm	30.162 mm	122.24 mm	76.2 mm	
Centroid Y	50.8 mm	355.6 mm	660.4 mm	965.2 mm	501.47 mm				499.92 mm	500. mm
Centroid Z	-76.198 mm				-122.24 mm		-30.161 mm	-30.162 mm	-76.2 mm	
Moment of Inertia Ip1	520.05 kg·mm²	519.98 kg·mm²	520.04 kg·mm²	520.05 kg·mm²	71194 kg·mm²	71187 kg·mm²	71209 kg·mm²	71186 kg·mm²	4.2426e+006 kg·mm²	1.0784e+005 kg·mm²
Moment of Inertia Ip2	1037.3 kg·mm²				18.904 kg·mm²	18.901 kg·mm²	18.913 kg·mm²	18.901 kg·mm²	1.9213e+005 kg·mm²	9817.1 kg·mm²
Moment of Inertia Ip3	519.99 kg·mm²	520.05 kg·mm²	519.98 kg·mm²	519.99 kg·mm²	71194 kg·mm²	71187 kg·mm²	71209 kg·mm²	71186 kg·mm²	4.2426e+006 kg·mm²	1.0784e+005 kg·mm²
Statistics										
Nodes	2277	2280	2238	2276	2539	2582	2693	2661	53357	15849
Elements	1144	1143	1109	1137	1128	1141	1204	1206	33526	7738
Mesh Metric	None									

4.3.2 Coordinate System

Coordinate systems presents in ANSYS play a vital role in modeling and in results identifications. The coordinate system is used for:

- To align the objects in ANSYS.
- Orthotropic material input.
- Loads input on certain faces of the surface effect elements.
- Input for boundary conditions, such as supports.
- Output of quantities, such as stresses, strains, and thermal gradients.

In this project the coordinate system was set to default; global as shown in table 3.

Table 3. ANSYS Coordinate system for analysis

Model (A4) > Coordinate Systems > Coordinate System

Object Name	*Global Coordinate System*
State	Fully Defined
Definition	
Type	Cartesian
Coordinate System ID	0.
Origin	
Origin X	0. mm
Origin Y	0. mm
Origin Z	0. mm
Directional Vectors	
X Axis Data	[1. 0. 0.]
Y Axis Data	[0. 1. 0.]
Z Axis Data	[0. 0. 1.]

4.3.3 Material Assignement

After creating geometry of the model, we need to assign materials to each and every component of the model. ANSYS Workbench has its own material library having a wide range of material types. Material models are created for the steel, concrete and Polyurea.

4.3.3.1 Polyurea

Moonie-Rivlin 9-Parameter equation for hyper elastic materials is used to model Polyurea with empirical material constants as shown in table 4. The stress curve for Polyurea is shown

in figure. The value of density and ultimate tensile strength for Polyurea is 1000 kg/m^3 and 19.2 MPa respectively. All the values are considered for standard room temperature; 22^{o}C.

Table 4. Empirical Constants for Polyurea

Material Constant C10	12.369	MPa
Material Constant C01	8.124	MPa
Material Constant C20	7.274	MPa
Material Constant C11	-17.653	MPa
Material Constant C02	3.062	MPa
Material Constant C30	0.043	MPa
Material Constant C21	-0.437	MPa
Material Constant C12	-0.298	MPa
Material Constant C03	2.94	MPa
Incompressibility Parameter D1	0	MPa^-1

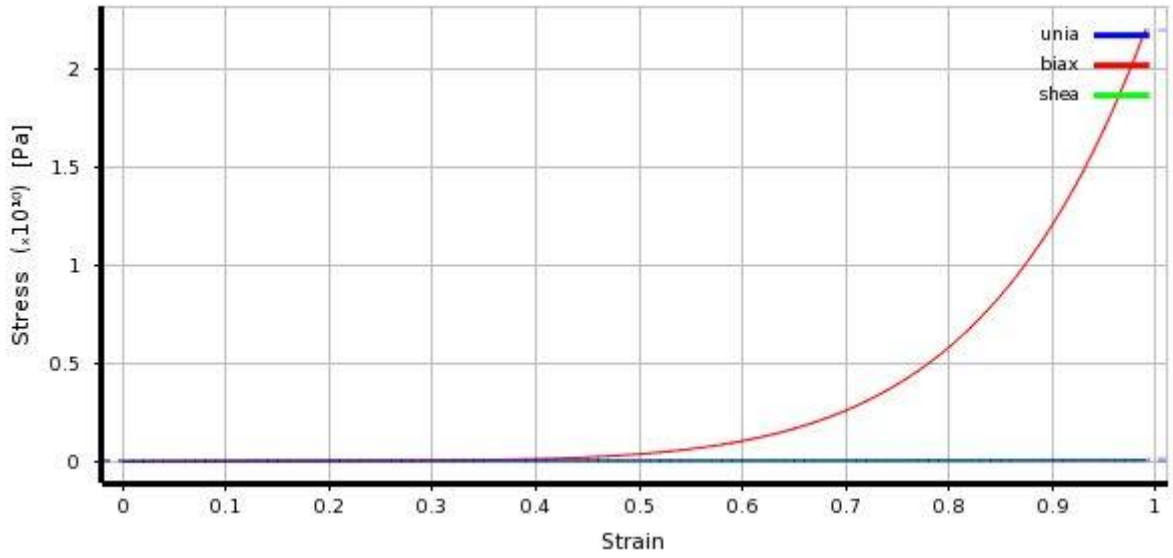

Figure 18. Stress-Strain relationship for Polyurea

4.3.3.2 Reinforcing Steel

The steel is modeled by isotropic elasticity based on Young's modulus, E=29000 ksi and poisson's ratio ν=0.3 for elastic region and multi-linear isotropic hardening based on the plastic stress-strain relationship for plastic region of the stress strain curve. The density of steel is used as 7850kg/m^3. Yield stress and ultimate stress for 280 MPa steel is 280 MPa and 420 MPa, respectively. Similarly, yield stress and ultimate stress for 420 MPa steel is 420

MPa and 620 MPa, respectively. Plastic stress strain relationship for the steels is given in figure 19 and 20.

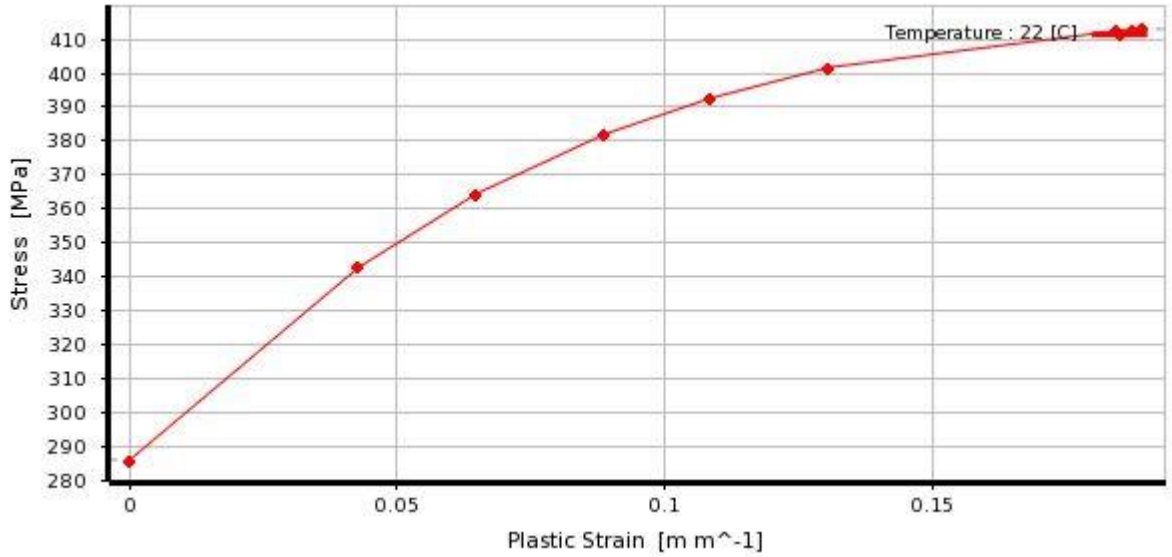

Figure 19. Plastic stress-strain relationship for 280MPa steel

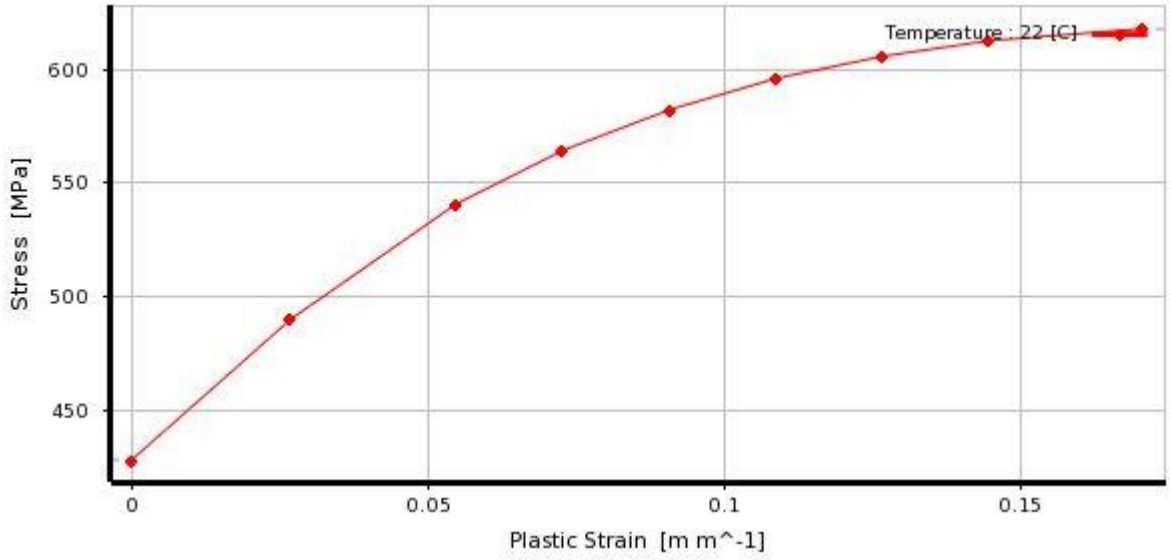

Figure 20. Plastic stress-strain relationship for 420 MPa steel

4.3.3.3 Concrete

The concrete is also modeled by isotropic elasticity based on Young's modulus and poisson's ratio for elastic region and multi-linear isotropic hardening based on the plastic stress-strain relationship for plastic region of the stress strain curve. The value of density for concrete is used as 2200 kg/m^3 and 2300 kg/m^3 for 28 MPa and 55 MPa concrete, respectively. Modulus

of elasticity of 28 MPa concrete is found to be 3604 ksi and poisson's ratio is 0.2. Compressive yield stress and ultimate stress for 28 MPa concrete is 12.4 MPa and 27.6 MPa, respectively while tensile yield stress and ultimate stress is 1.1 MPa and 2.76 Mpa. Plastic stress strain relationship for the concrete is given in figure 21.

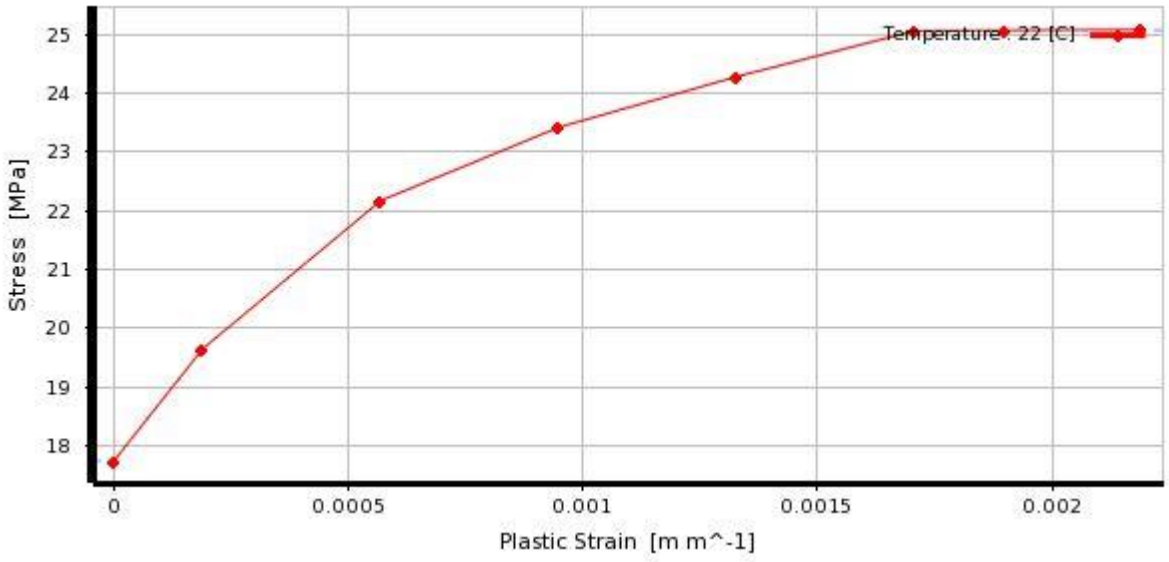

Figure 21. Plastic stress-strain relationship for 28 MPa concrete

4.3.4 Connections / Contacts

The existing types of contact present in ANSYS are listed below. These types of cantact apply to interaction regions made up of surfaces only.

Bonded

This is the default configuration and applies to all contact regions (surfaces, solids, lines, faces, edges). If contact regions are bonded, then no sliding or separation between faces or edges is allowed. The region behave like it is glued. This type of contact allows for a linear solution since the contact length/area will not change during the application of the load. If contact is determined on the mathematical model, any gaps will be closed and any initial penetration will be ignored.

Frictional

In this setting, the two contacting geometries can carry shear stresses up to a certain magnitude across their interface before they start sliding relative to each other. This state is known as "sticking." The model defines an equivalent shear stress at which sliding on the geometry begins as a fraction of the contact pressure. Once the shear stress is exceeded, the two geometries will slide relative to each other. The coefficient of friction can be any non-negative value.

Rough

Similar to the frictionless setting, these setting models perfectly rough frictional contact where there is no sliding. This case corresponds to an infinite friction coefficient between the contacting bodies. By default, no automatic closing of gaps is performed. It only applies to regions of faces (for 3D solids) or edges (for 2D plates).

Frictionless

This setting models standard unilateral contact; that is, normal pressure equals zero if separation occurs. A zero coefficient of friction is assumed, thus allowing free sliding. The model should be well constrained when using this contact setting. Thus gaps can form in the model between bodies depending on the loading. This solution is nonlinear because the area of contact may change as the load is applied.

The elements of RC Column were joined into a part and made a single object except the steel plate for load application at the top of the column, and imported in to ANSYS Workbench environment. The connections between the elements of RC column were "bonded" by default and the contact between the steel plate and RC column was designed to be "rough" so that there is no sliding on the contact face at larger deformations. Details are shown in table 4.

Model (A4) > Connections > Contacts > Contact Regions		
Object Name	*Rough - 4K2MM\Plate for Load Application To 4K2MM\Concrete*	*Rough - 4K2MM\Plate for Load Application To 4K2MM\Polyurea*
State	Fully Defined	
Scope		
Scoping Method	Geometry Selection	
Contact	1 Face	
Target	1 Face	
Contact Bodies	4K2MM\Plate for Load Application	
Target Bodies	4K2MM\Concrete	4K2MM\Polyurea
Definition		
Type	Rough	
Scope Mode	Automatic	
Behavior	Asymmetric	
Trim Contact	Program Controlled	
Trim Tolerance	2.6661 mm	
Suppressed	No	
Advanced		
Formulation	Augmented Lagrange	
Small Sliding	Off	
Detection Method	Nodal-Normal To Target	
Penetration Tolerance	Program Controlled	
Elastic Slip Tolerance	Program Controlled	
Normal Stiffness	Program Controlled	
Update Stiffness	Program Controlled	
Stabilization Damping Factor	0.	
Pinball Region	Program Controlled	
Time Step Controls	None	
Geometric Modification		
Interface Treatment	Add Offset, No Ramping	
Offset	0. mm	
Contact Geometry Correction	None	
Target Geometry Correction	None	

Table 5. Details of contact faces

4.3.5 Meshing

The results accuracy of finite element model depends upon the mesh size and the configuration of mesh the small size mesh generates more accurate results as compared to large size mesh. And adversely the small size mesh requires more computational time and other requirements. So the size of mesh should be selected carefully.

The mesh size function is set to adaptive with medium relevance center and high smoothing. The mesh method used in the study is tetrahedrons with patch conforming algorithm. Details of meshed elements and nodes are shown in table 5 and figure 22.

Model (A4) > Mesh	
Object Name	*Mesh*
State	Solved
Display	
Display Style	Body Color
Defaults	
Physics Preference	Mechanical
Relevance	0
Element Order	Program Controlled
Sizing	
Size Function	Adaptive
Relevance Center	Medium
Element Size	Default
Mesh Defeaturing	Yes
Defeature Size	Default
Transition	Fast
Initial Size Seed	Assembly
Span Angle Center	Medium
Bounding Box Diagonal	1066.40 mm
Minimum Edge Length	9.97460 mm
Quality	
Check Mesh Quality	Yes, Errors
Error Limits	Standard Mechanical
Target Quality	Default (0.050000)
Smoothing	High
Mesh Metric	None
Inflation	
Use Automatic Inflation	None
Inflation Option	Smooth Transition
Transition Ratio	0.272
Maximum Layers	5
Growth Rate	1.2
Inflation Algorithm	Pre
View Advanced Options	No
Advanced	
Number of CPUs for Parallel Part Meshing	Program Controlled
Straight Sided Elements	No
Number of Retries	Default (4)
Rigid Body Behavior	Dimensionally Reduced
Mesh Morphing	Disabled
Triangle Surface Mesher	Program Controlled
Topology Checking	No
Pinch Tolerance	Please Define
Generate Pinch on Refresh	No
Statistics	
Nodes	72648
Elements	51157

Model (A4) > Mesh > Mesh Controls	
Object Name	*Patch Conforming Method*
State	Fully Defined
Scope	
Scoping Method	Geometry Selection
Geometry	11 Bodies
Definition	
Suppressed	No
Method	Tetrahedrons
Algorithm	Patch Conforming
Element Order	Use Global Setting

Table 6. Details of meshing of elements and nodes

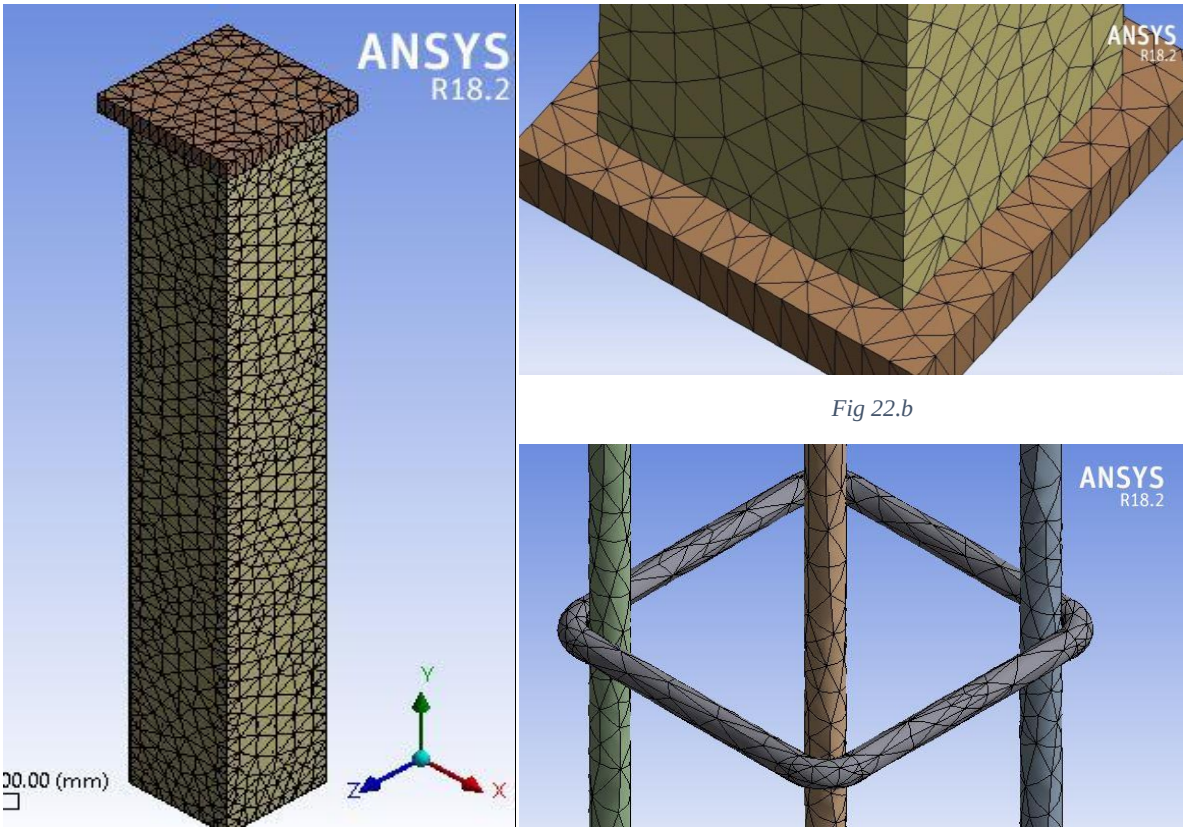

Fig 22.a *Fig 22.b* *Fig 22.c*

Figure 22. Details of meshing of RC column

4.3.6 Analysis Type: Static Structural

ANSYS is general purpose finite element software which have multiple options for the analysis of the finite element model. In lieu of physical model which was tested under the static cyclic axial loads, the static structural analysis type was selected for the numerical model creation and solution. In this software there are many solver options. Mechanical APDL solver was selected in this study for the static structural analysis.

4.3.6.1 Analysis settings

The settings used in the analysis are listed Table 7 and Table 8. Table 7 shows the details of step controls, solver controls, output control, nonlinear control etc., table 8 show the details of sub steps. The cyclic loading was divided in 40 steps. For the successful convergence of force and displacement, the number of sub steps was increased with carry over time step.

Table 7. Analysis settings mechanical APDL solver

Model (A4) > Static Structural (A5) > Analysis Settings	
Object Name	*Analysis Settings*
State	Fully Defined
Restart Analysis	
Restart Type	Program Controlled
Load Step	25
Substep	47
Time	10072 s
Step Controls	
Number Of Steps	40.
Current Step Number	1.
Step End Time	60. s
Auto Time Stepping	On
Define By	Substeps
Initial Substeps	50.
Minimum Substeps	30.
Maximum Substeps	70.
Solver Controls	
Solver Type	Program Controlled
Weak Springs	Off
Solver Pivot Checking	Program Controlled
Large Deflection	On
Inertia Relief	Off
Rotordynamics Controls	
Coriolis Effect	Off
Restart Controls	
Generate Restart Points	Program Controlled
Retain Files After Full Solve	No
Combine Restart Files	Program Controlled
Nonlinear Controls	
Newton-Raphson Option	Program Controlled
Force Convergence	Program Controlled
Moment Convergence	Program Controlled
Displacement Convergence	Program Controlled
Rotation Convergence	Program Controlled
Line Search	Program Controlled
Stabilization	Off
Output Controls	
Stress	Yes
Strain	Yes
Nodal Forces	No
Contact Miscellaneous	No
General Miscellaneous	No
Store Results At	All Time Points
Analysis Data Management	
Solver Files Directory	D:\1.MS Thesis Yasir Siraj\New\Ansys\My Thesis\My Work_files\dp0\SYS\MECH\
Future Analysis	None
Scratch Solver Files Directory	
Save MAPDL db	No
Delete Unneeded Files	Yes
Nonlinear Solution	Yes
Solver Units	Active System
Solver Unit System	nmm

Table 8. Details of substeps for analysis

Model (A4) > Static Structural (A5) > Analysis Settings
Step-Specific "Step Controls"

Step	Step End Time	Initial Substeps	Minimum Substeps	Maximum Substeps	Carry Over Time Step
1	60. s	50.			
2	120. s				
3	240. s				
4	360. s				
5	540. s		30.	70.	
6	720. s				
7	960. s				
8	1200. s				
9	1500. s				
10	1800. s				
11	2160. s				
12	2520. s				
13	2940. s				On
14	3360. s				
15	3840. s				
16	4320. s				
17	4860. s		50.	100.	
18	5400. s				
19	6000. s				
20	6600. s				
21	7260. s				
22	7920. s				
23	8640. s				
24	9360. s				
25	10140 s				
26	10920 s				
27	11760 s				
28	12600 s				
29	13500 s				
30	14400 s				
31	15360 s				
32	16320 s				
33	17340 s				
34	18360 s				
35	19440 s		100.	150.	
36	20520 s				
37	21660 s				
38	22800 s				
39	24000 s				
40	25200 s				

4.3.6.2 Boundary conditions

Boundary conditions include loadings and support conditions. Displacements are used for the application of cyclic loading and the support of the column is assumed as fixed support to restrict displacement in all directions. Figure 23 shows the loading and boundary condition applied to the finite element model. The axial load was applied as a directional displacement only in Y axis as a function of time on the top face of the steel plate with restrictions in X and Z axes. Figure 24 shows the cyclic loading.

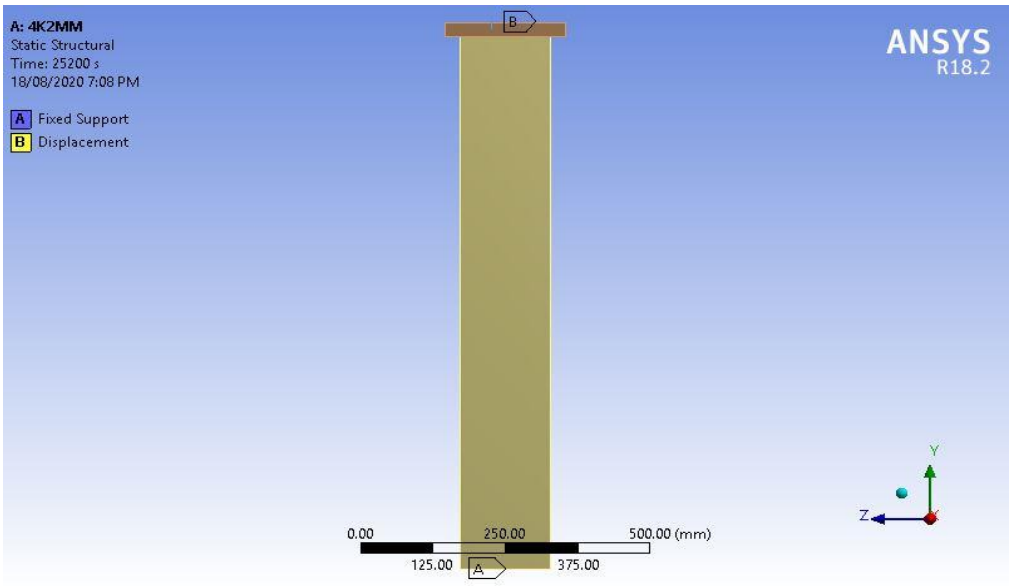

Figure 23. Boundary conditions for RC column

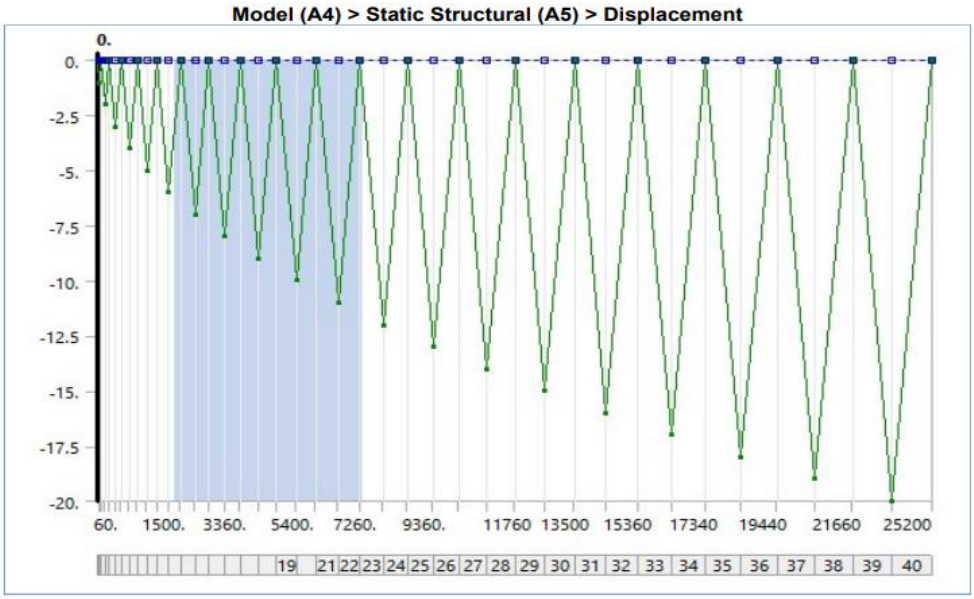

Figure 24. Displacement applied on RC column

4.3.7 FE Solution

In this section the output required for the analysis are discussed. In lieu of scope of this study: the force and displacement in longitudinal direction (Y axis) are selected for the comparison to compare the effectiveness of Polyurea confinement for reinforced concrete columns. User defined output is selected for directional displacement (uy) and direction force reaction (fy). These two outputs are used for plotting and comparison of Force-Displacement curves for each RC column. Figure 25 shows max deformation in RC column upon loading and loading. Object separation at the contact can be observed and for that reason the contact surface was modeled to be rough, so that the column may retain its residual displacements upon unloading. Force-Displacement curve is shown in figure 26.

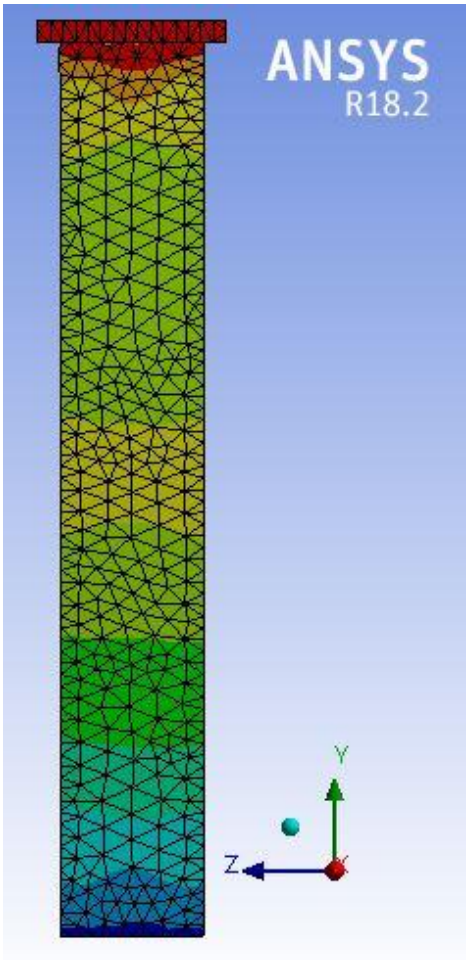

Fig 25(a). Deformation in loading phase

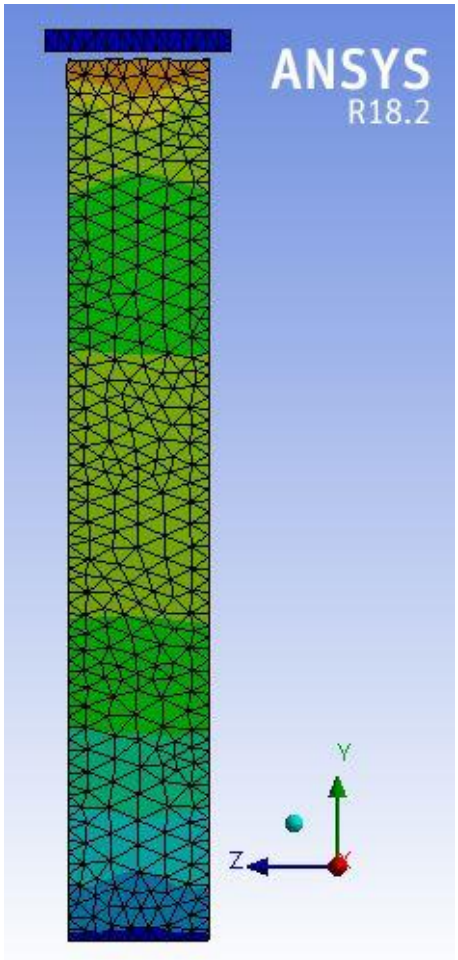

Fig 25(b). Deformation in unloading phase

Figure 25. Deformation in column during loading and unloading phase

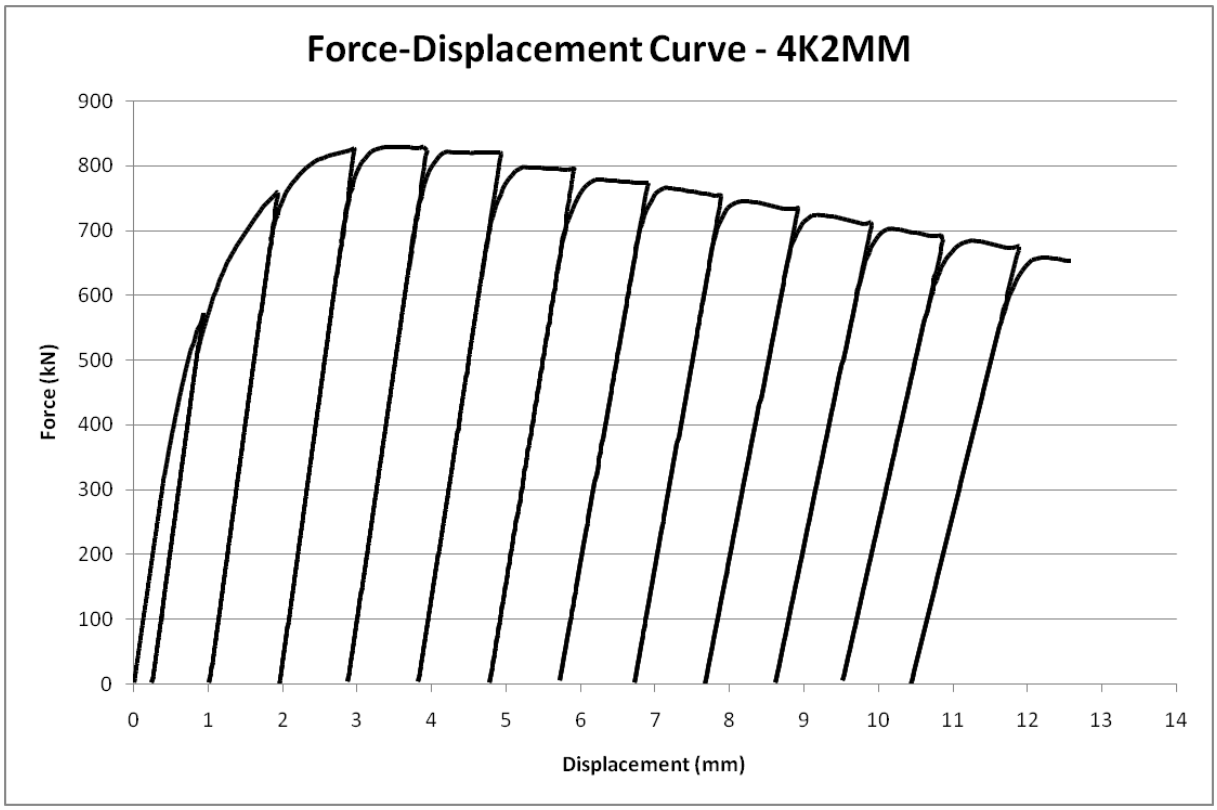

Figure 26. Force-Displacement curve for 4K2MM

CHAPTER 5

ANALYSIS AND RESULTS

In this chapter the results obtained from ANSYS for each RC column will be compared and analyzed. The effectiveness of confinement using Polyurea will be analyzed with different parameters. For comparison, gain and loss of a specific parameter for RC column will be discussed. Parameter wise comparisons will be made for 28 MPa as well as 55 MPa RC columns confined with Polyurea in various thicknesses of 2mm, 4mm and 6mm with control sample having no confinement. The following parameters are used for comparison in this study.

1. Force - Displacement relationship
2. Yield, ultimate and rupture load and displacement
3. Energy dissipation
4. Ductility

5.1 Force - Displacement Relationship

The Force-Displacement and backbone curves obtained from the hysteresis loops of the RC columns having concrete compressive strength of 28 MPa and 55 MPa are discussed in this section. It is observed that the performance of RC columns due to confinement of Polyurea is enhanced and gave a higher peak load and rupture loads and displacements and exhibits better ductile response. The better performance of RC columns is due to the fact that it has withstood additional number of cycles before reaching failure point. The comparison of hysteresis response is done as area under the backbone curve. It can be seen that RC columns confined with Polyurea depicted larger energy dissipation, which is actually the work done or area under the curve. This was possible because of relatively better post peak response.

Force-Displacement and backbone curves for 28 MPa are presented in figure 27 to figure 30, and for 55 MPa are presented in figure 31 to figure 34.

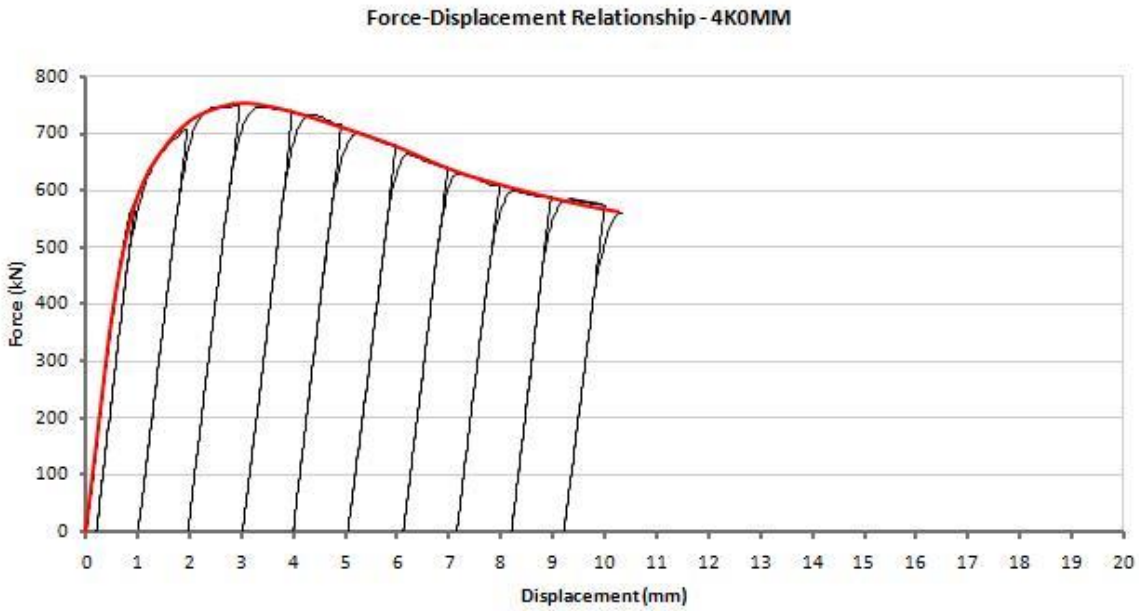

Figure 27. Force-Displacement relationship - 4K0MM

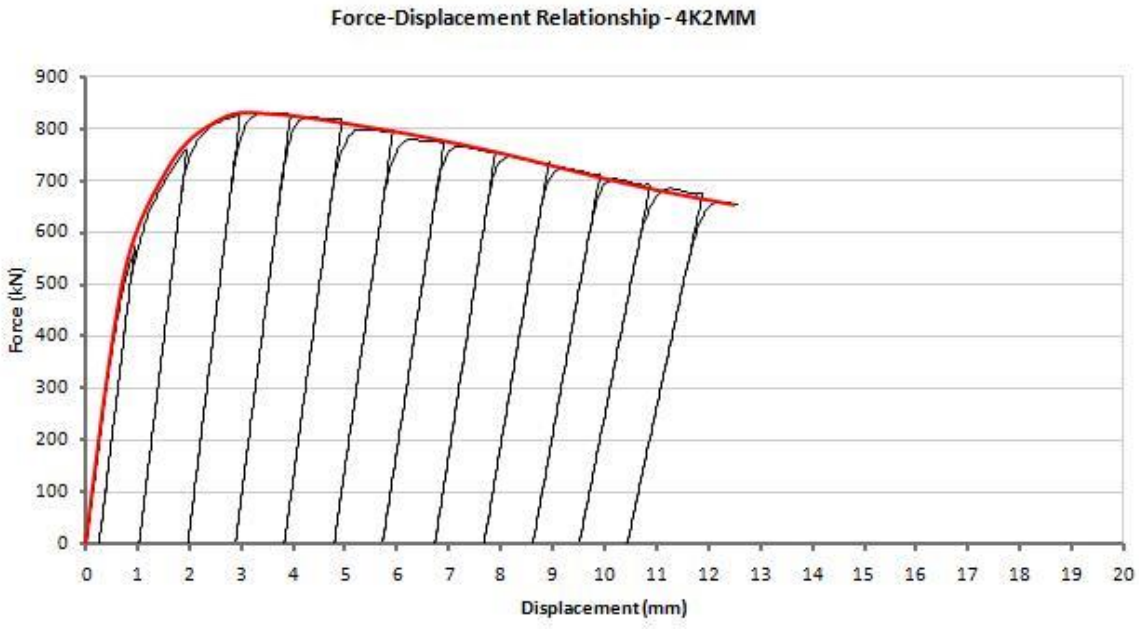

Figure 28. Force-Displacement relationship - 4K2MM

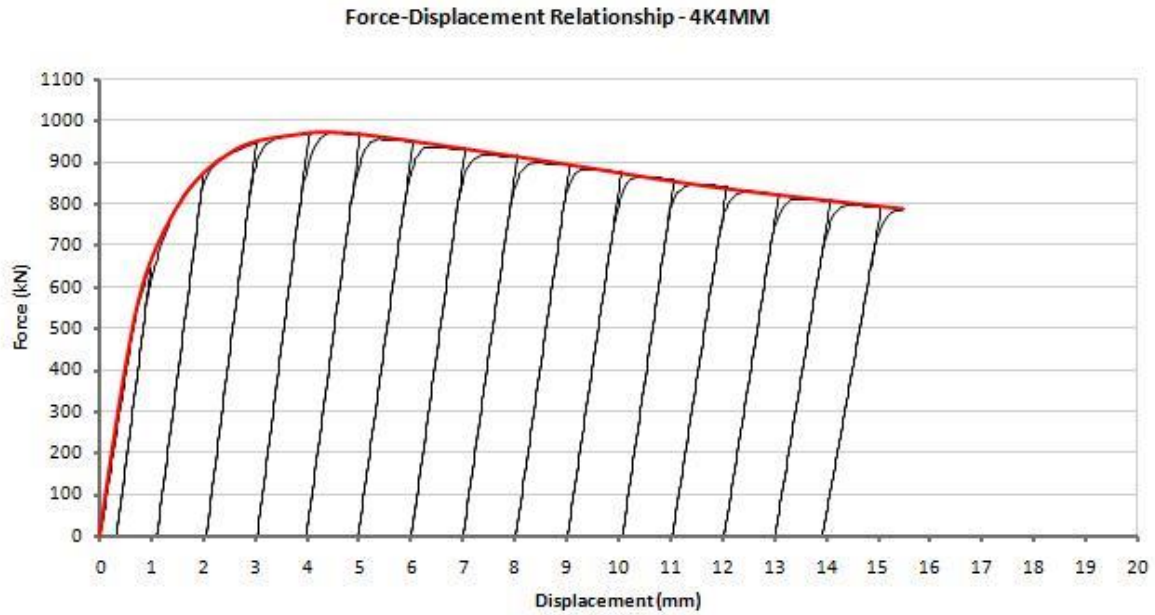

Figure 29. Force-Displacement relationship 4K4MM

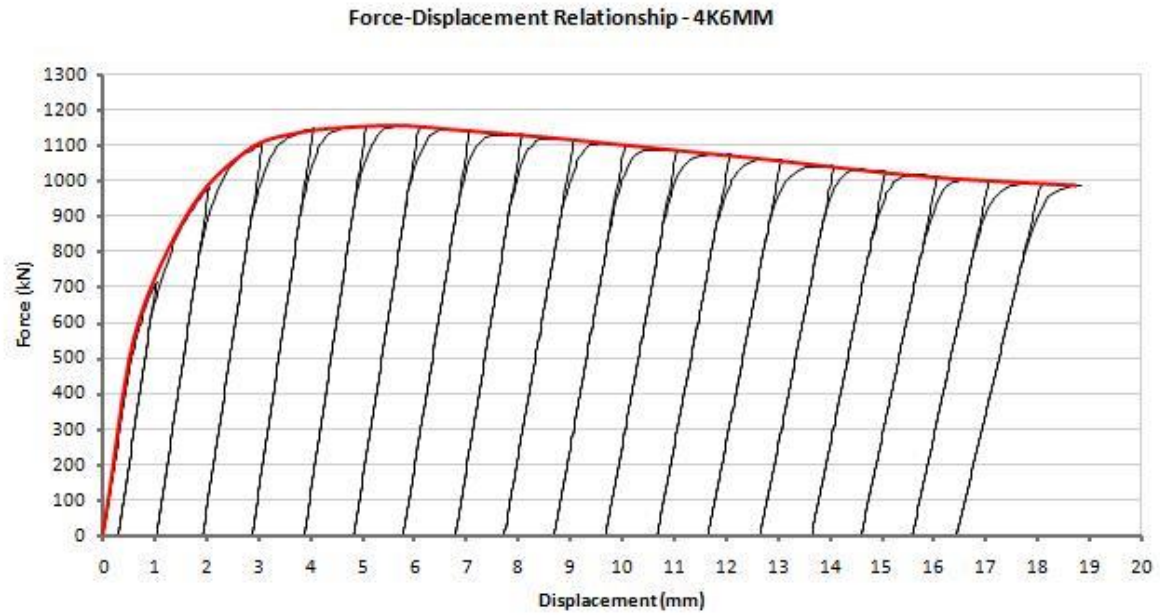

Figure 30. Force-Displacement relationship 4K6MM

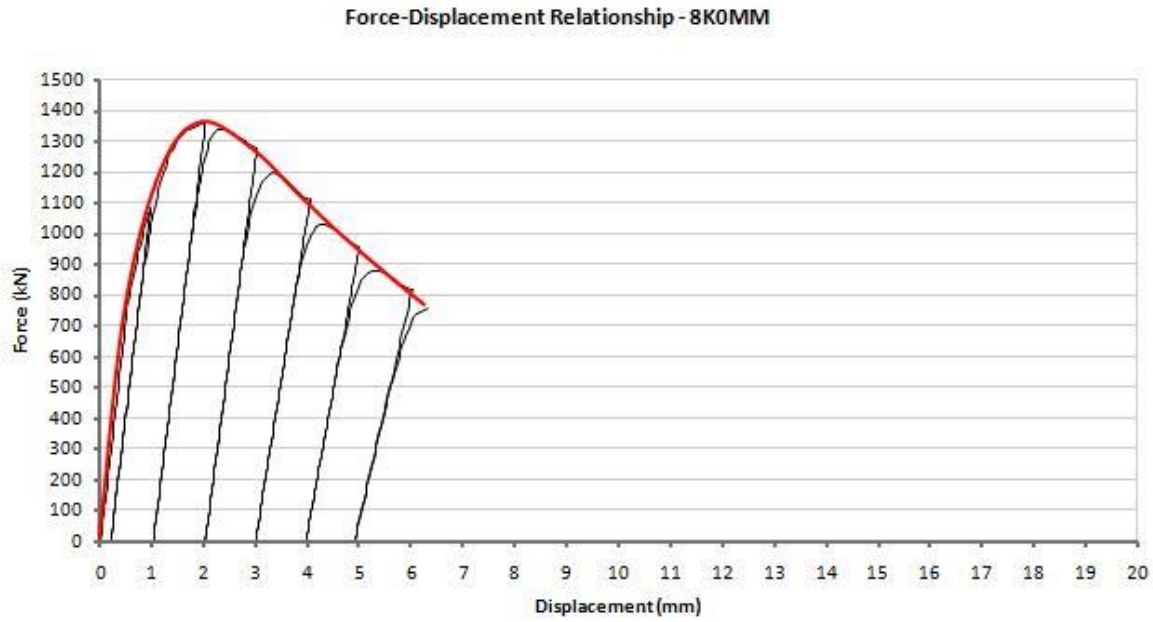

Figure 31. Force-Displacement relationship 8K0MM

Figure 32. Force-Displacement relationship 8K2MM

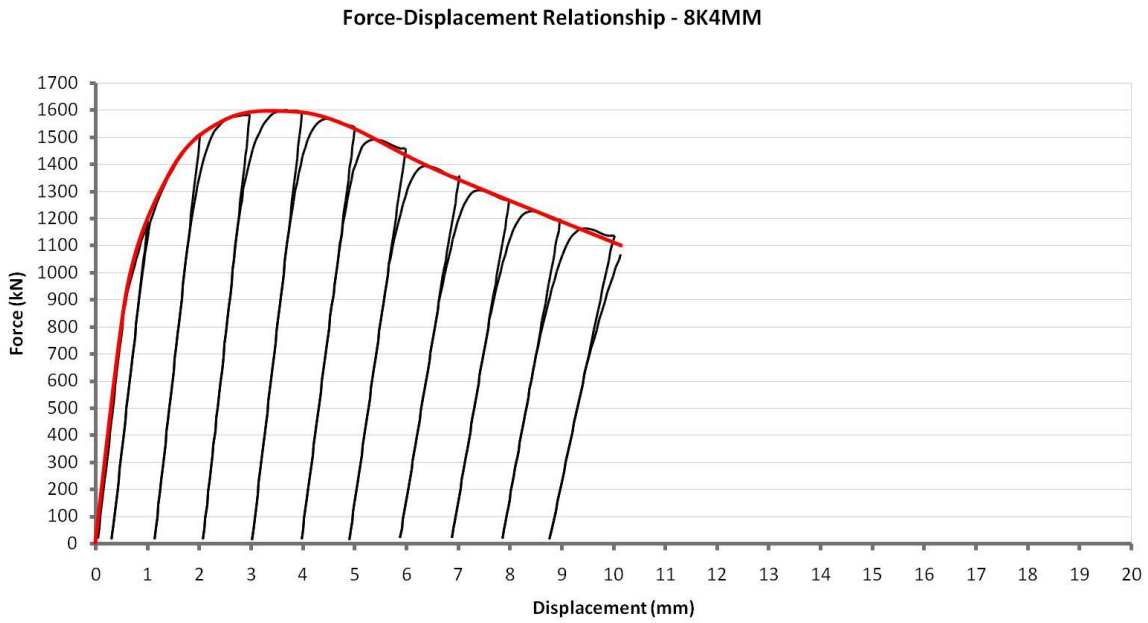

Figure 33. Force-Displacement relationship 8K4MM

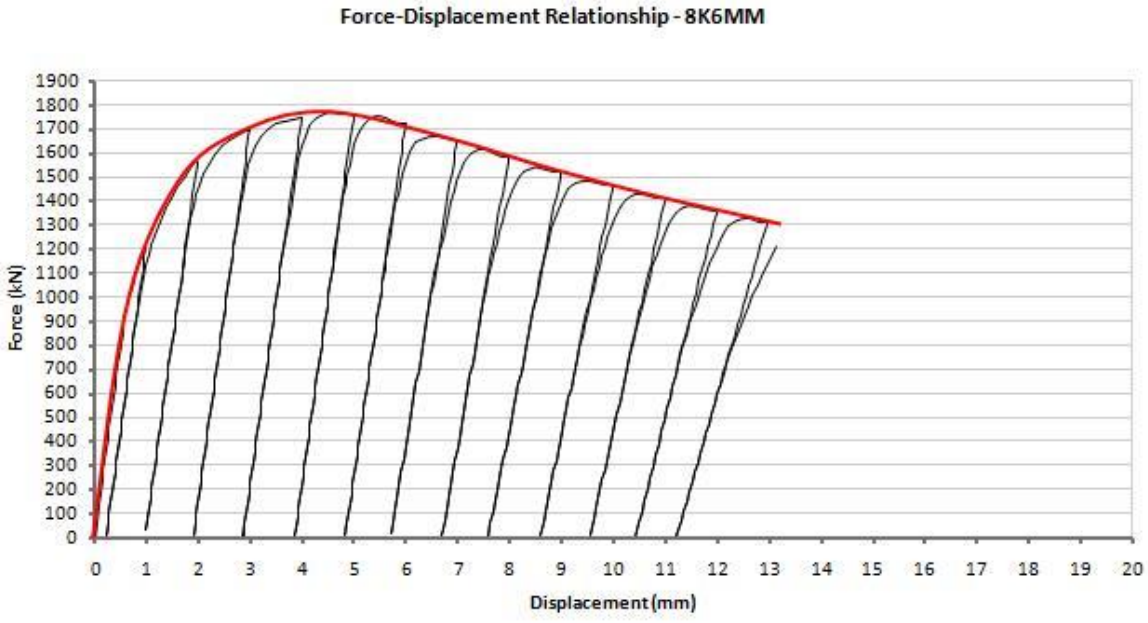

Figure 34. Force-Displacement relationship 8K6MM

5.2 Yield, Ultimate and Rupture Load and Displacement

In this section yield, ultimate and rupture load and displacement comparison is discussed for RC columns. Comparison of yield point, peak point and rupture point for 28 MPa is shown in table 9 and for 55 MPa is given in table 10.

5.2.1 Comparison for 28 MPa

Yield Point: The enhancement in yield load capacity of columns due to 2mm, 4mm and 6mm confinement is 9.71%, 29.82% and 51.04% respectively and displacement at the yield load is increased by 13.76%, 36.24% and 62.42%.

Peak Point: Similarly, the peak load capacity of columns is increased by 10.83%, 29.95% and 54.28% and displacement at the peak load is increased by 14.86%, 41.62% and 68.98%.

Rupture Point: The load at failure point is increased by 16.40%, 40.11% and 75.40% and displacement at failure point is increased by 21.78%, 50.24% and 82.58%.

5.2.2 Comparison for 55 MPa

Yield Point: The enhancement in yield load capacity of columns due to 2mm, 4mm and 6mm confinement is 5.68%, 16.72% and 31.70%, respectively and displacement at the yield load is increased by 14.51%, 37.50% and 55.69%.

Peak Point: Similarly, the peak load capacity of columns is increased by 8.38%, 19.76% and 32.26% and displacement at the peak load is increased by 45.27%, 88.56% and 127.86%

Rupture Point: The load at failure point is increased by 30.03%, 41.27% and 59.92% and displacement at failure point is increased by 22.58%, 61.05% and 109.06%.

Table 9. Comparison of yield point, peak point and rupture point for 28 MPa

Sample	YIELD POINT		PEAK POINT		RUPTURE POINT	
	Displacement (mm)	Force (kN)	Displacement (mm)	Force (kN)	Displacement (mm)	Force (kN)
4K0MM	1.99	721	2.98	748	10.33	561
4K2MM	2.26	791	3.39	829	12.58	653
4K4MM	2.71	936	4.06	972	15.52	786
4K6MM	3.23	1089	4.84	1154	18.86	984

Table 10. Comparison of yield point, peak point and rupture point for 55 MPa

Sample	YIELD POINT		PEAK POINT		RUPTURE POINT	
	Displacement (mm)	Force (kN)	Displacement (mm)	Force (kN)	Displacement (mm)	Force (kN)
8K0MM	1.70	1268	2.01	1336	6.29	756
8K2MM	1.95	1340	2.92	1448	7.71	983
8K4MM	2.43	1480	3.79	1600	10.13	1068
8K6MM	3.05	1670	4.58	1767	13.15	1209

5.3 Ductility

Ductility index of different samples was calculated from displacement at their yield point and ultimate point. Ductility index is referred as the ratio of displacements at ultimate point and yield point. Comparison of ductility of RC columns for 28 MPa and 55 MPa is given in table 11. It is observed that ductility index is significantly enhanced for RC columns with confinement.

Table 11. Comparison of ductility index for 28 MPa and 55 MPa

Sample	Yield Displacement (mm)	Ultimate Displacement (mm)	Ductility Index	% Increase in Ductility
4K0MM	1.99	10.33	5.20	-
4K2MM	2.26	12.58	5.57	7.1
4K4MM	2.71	15.52	5.73	10.3
4K6MM	3.23	18.86	5.85	12.4

Table 12. Comparison of ductility index for 55 MPa

Sample	Yield Displacement (mm)	Ultimate Displacement (mm)	Ductility Index	% Increase in Ductility
8K0MM	1.70	6.29	3.70	-
8K2MM	1.95	7.71	3.96	7.0
8K4MM	2.43	10.13	4.17	12.7
8K6MM	3.05	13.15	4.31	16.4

5.4 Energy Dissipation

Hysteresis response of RC columns under cyclic loading is used for calculation of energy dissipation in loading and unloading for each cycle. The area enclosed in a hysteresis loop is the total energy dissipated in that cycle. The energies are computed from hysteresis loops by calculation of area under the loading and unloading curves. The area under the unloading curve is subtracted from the area of the loading curve, which gives the amount of total energy dissipated in the cycle. The amounts of energies dissipated by different samples are presented in figure 35 to figure 42. Maximum energy dissipated by each sample is presented in

figure 43 & 44 and compared in Table 13 to 15. It is pertinent to mention that due to improved post peak behavior of RC columns confined with Polyurea, there is a remarkable enhancement in their energy dissipation capacity.

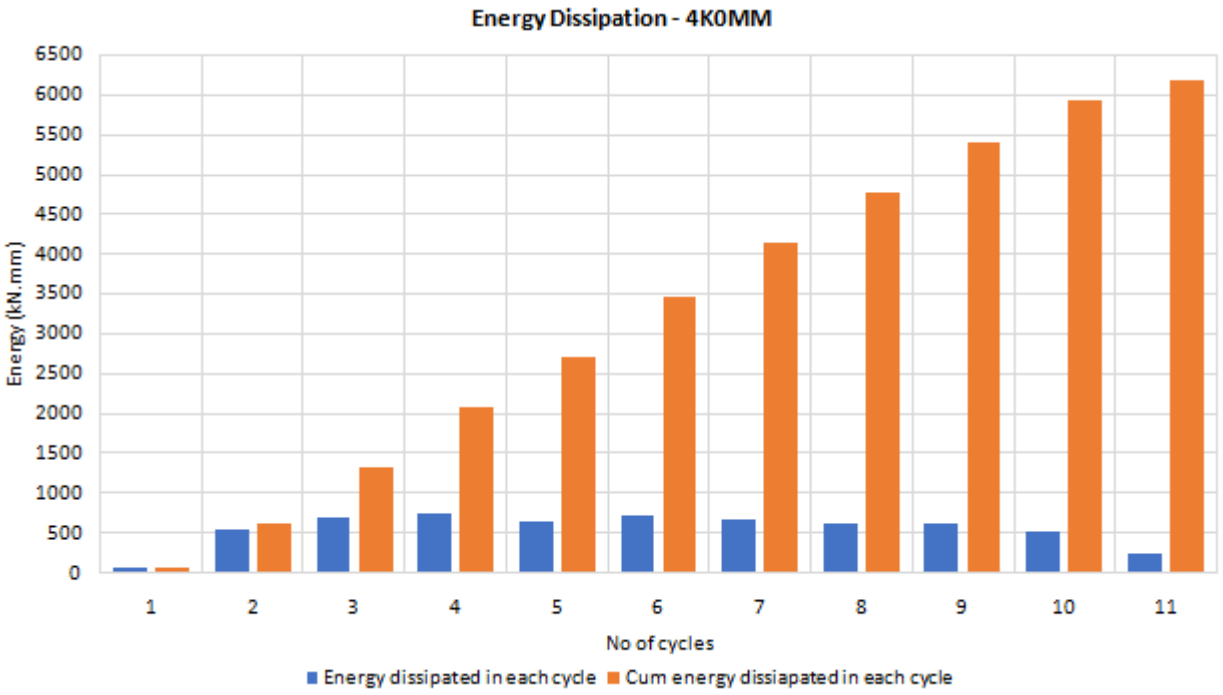

Figure 35. Energy Dissipation in 4K0MM

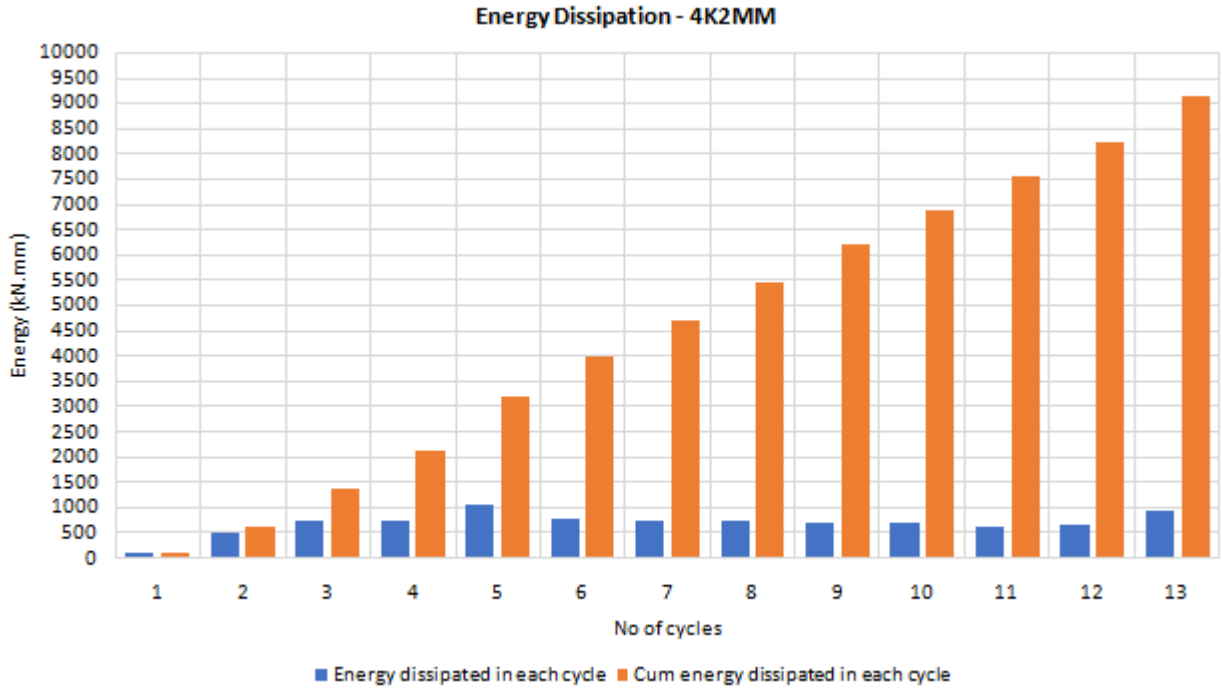

Figure 36. Energy Dissipation in 4K2MM

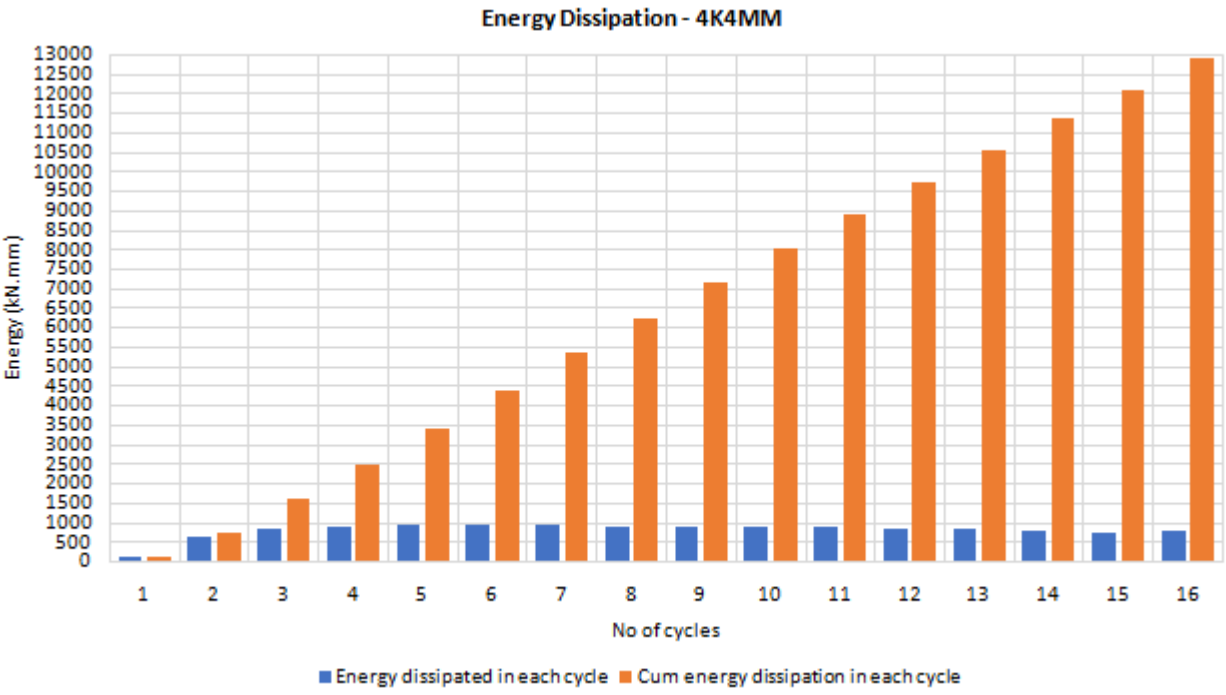

Figure 37. Energy Dissipation in 4K4MM

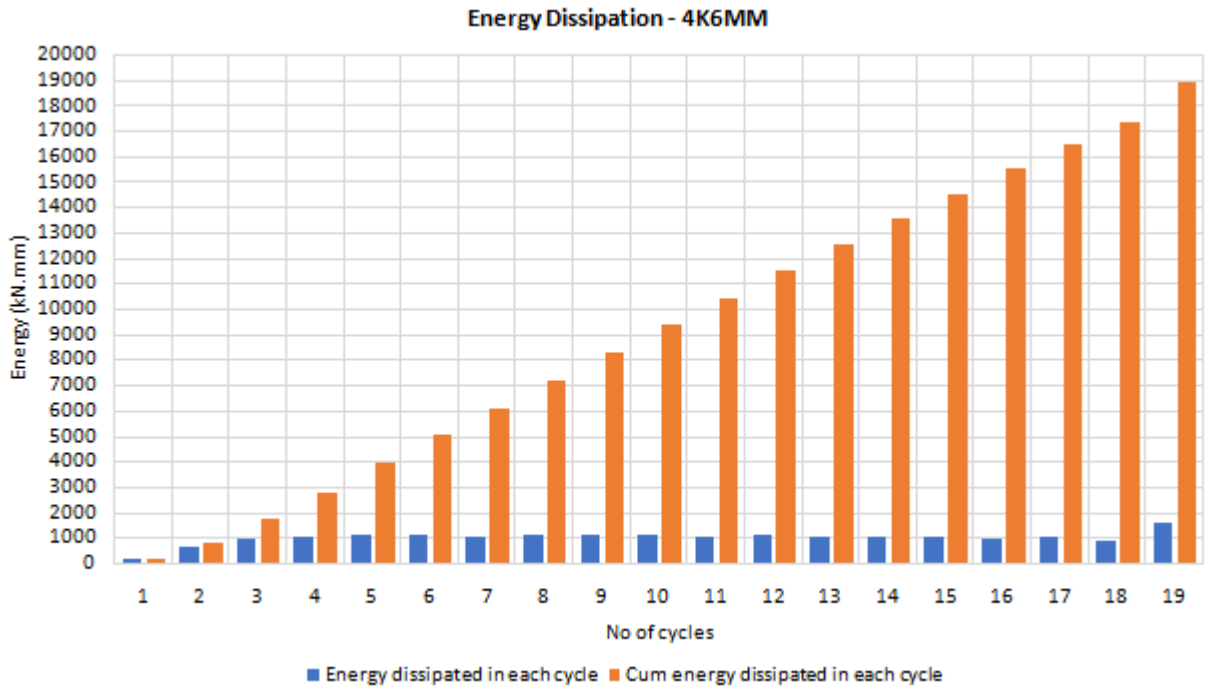

Figure 38. Energy Dissipation in 4K6MM

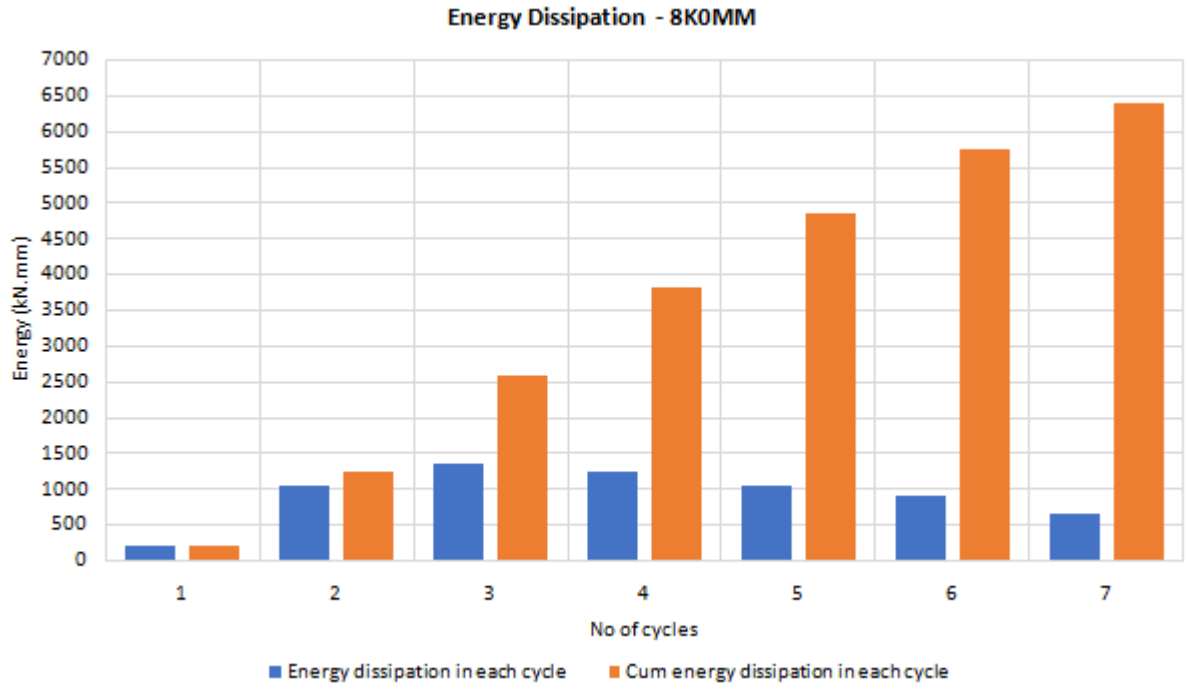

Figure 39. Energy Dissipation in 8K0MM

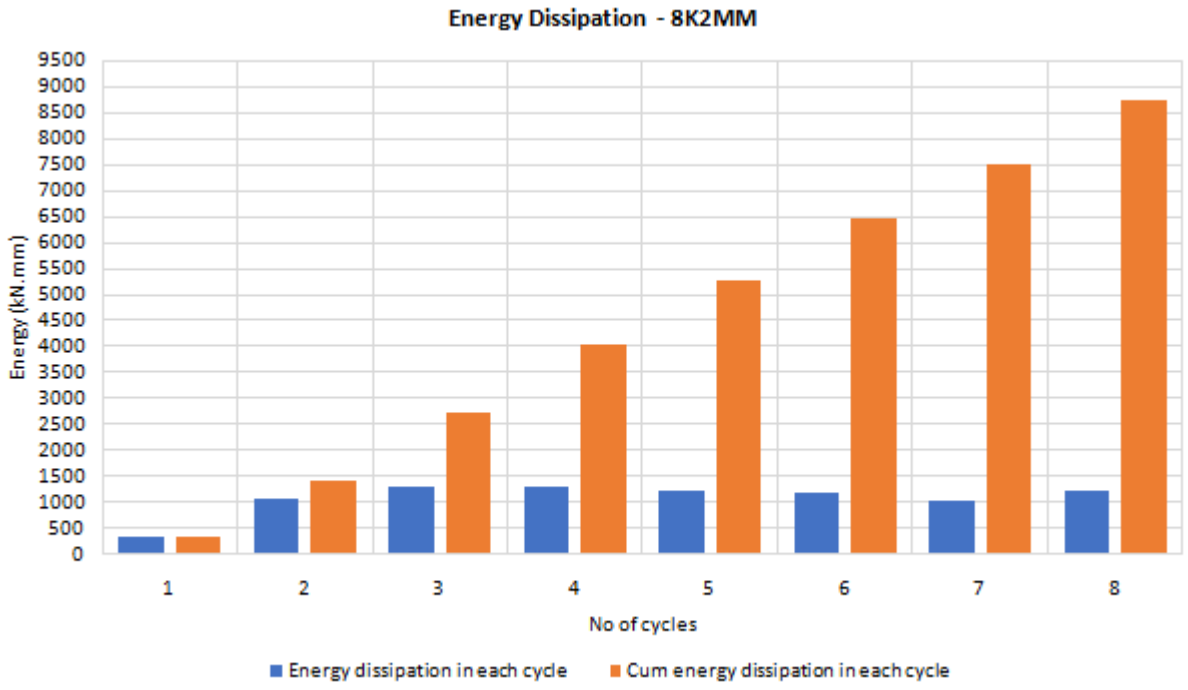

Figure 40. Energy Dissipation in 8K2MM

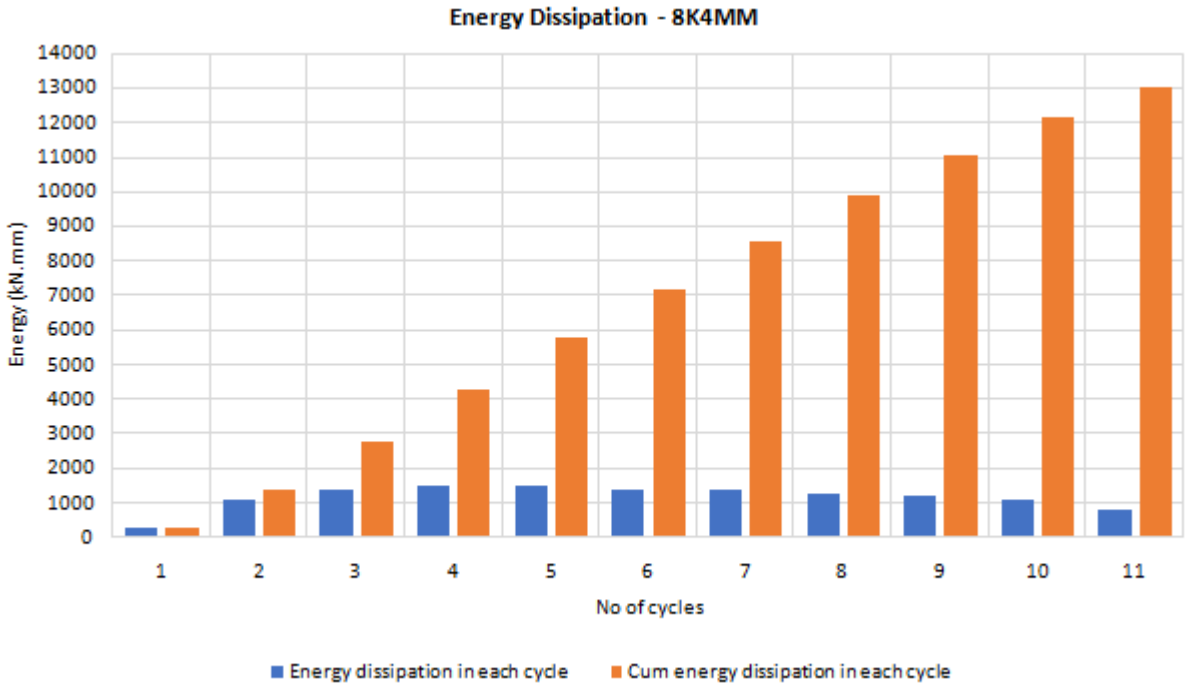

Figure 41. Energy Dissipation in 8K4MM

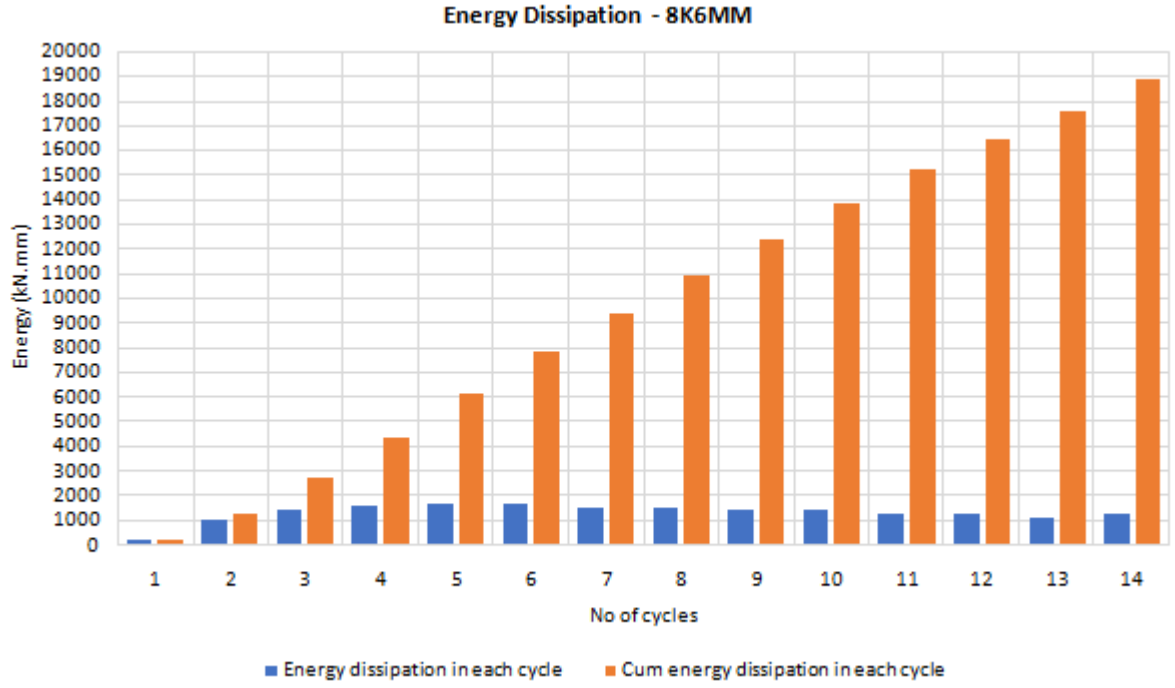

Figure 42. Energy Dissipation in 8K6MM

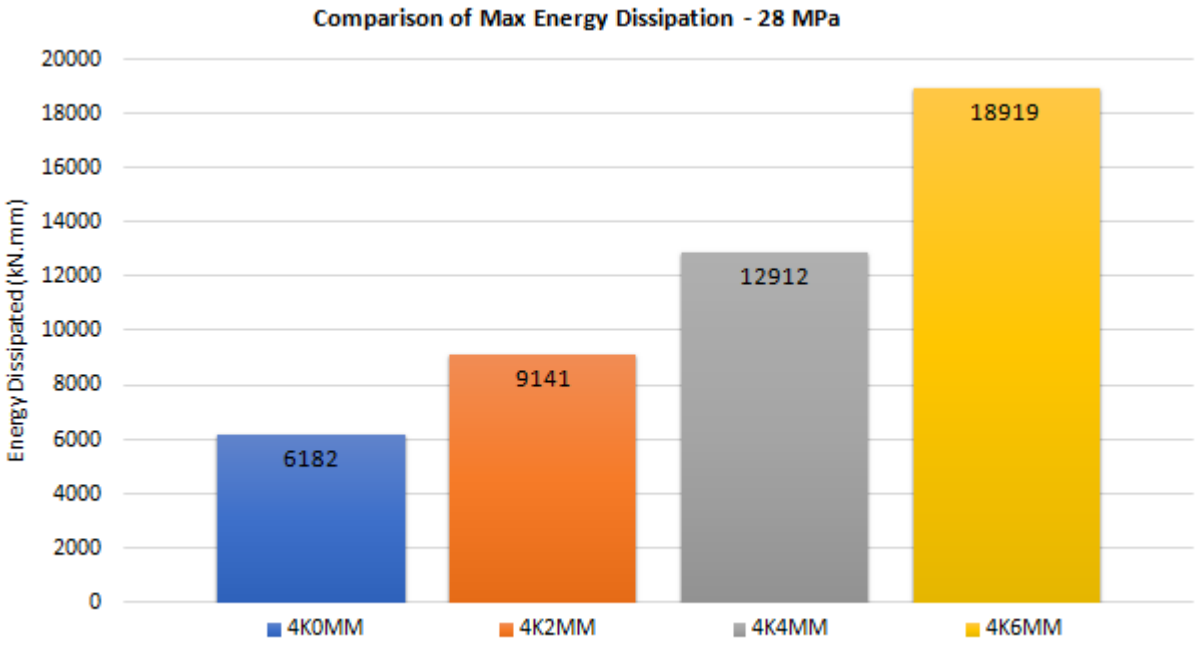

Figure 43. Comparison of Max energy dissipated for 28 MPa

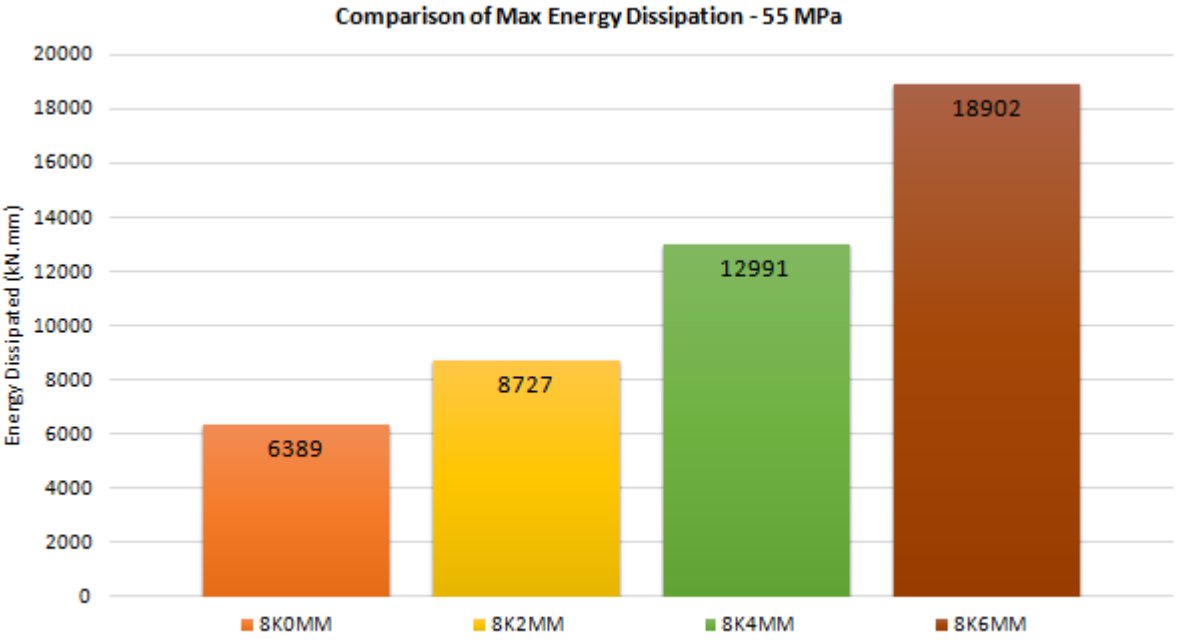

Figure 44. Comparison of max energy dissipation for 55 MPa

Table 13. Energy dissipation in each cycle for 28 MPa

No of Cycle	4K0MM		4K2MM		4K4MM		4K6MM	
	Energy dissipated in each cycle (kN.mm)	Cum energy dissipated in each cycle (kN.mm)	Energy dissipated in each cycle (kN.mm)	Cum energy dissipated in each cycle (kN.mm)	Energy dissipated in each cycle (kN.mm)	Cum energy dissipated in each cycle (kN.mm)	Energy dissipated in each cycle (kN.mm)	Cum energy dissipated in each cycle (kN.mm)
1	86.474	86.474	120.158	120.158	143.357	143.357	182.145	182.145
2	539.688	626.162	512.122	632.280	609.690	753.048	622.566	804.711
3	699.106	1325.268	754.171	1386.451	846.175	1599.222	922.990	1727.701
4	751.687	2076.955	735.298	2121.749	902.639	2501.861	1034.981	2762.682
5	641.793	2718.748	1080.232	3201.982	928.254	3430.115	1135.769	3898.451
6	735.811	3454.558	779.093	3981.075	958.165	4388.280	1110.272	5008.723
7	679.617	4134.176	737.289	4718.363	954.057	5342.337	1047.858	6056.580
8	637.633	4771.809	751.676	5470.039	896.498	6238.835	1131.494	7188.074
9	621.541	5393.350	717.564	6187.603	898.834	7137.669	1075.416	8263.490
10	525.316	5918.666	701.716	6889.318	869.098	8006.767	1069.874	9333.364
11	263.260	6181.926	650.011	7539.329	886.945	8893.712	1046.007	10379.371
12			662.741	8202.070	847.950	9741.662	1087.485	11466.856
13			938.933	9141.003	815.030	10556.692	1037.436	12504.292
14					804.581	11361.274	1017.946	13522.239
15					749.476	12110.750	989.824	14512.063
16		-		-	801.040	12911.790	973.282	15485.345
17							988.601	16473.946
18						-	886.179	17360.124
19							1558.469	18918.593

Table 14. Energy dissipation in each cycle for 55 MPa

No of Cycle	8K0MM		8K2MM		8K4MM		8K6MM	
	Energy dissipated in each cycle (kN.mm)	Cum energy dissipated in each cycle (kN.mm)	Energy dissipated in each cycle (kN.mm)	Cum energy dissipated in each cycle (kN.mm)	Energy dissipated in each cycle (kN.mm)	Cum energy dissipated in each cycle (kN.mm)	Energy dissipated in each cycle (kN.mm)	Cum energy dissipated in each cycle (kN.mm)
1	202.157	202.157	333.799	333.799	272.226	272.226	245.258	245.258
2	1035.270	1237.428	1088.296	1422.095	1122.104	1394.330	1036.560	1281.818
3	1334.605	2572.032	1303.727	2725.821	1364.474	2758.804	1493.523	2775.341
4	1232.575	3804.607	1320.892	4046.714	1501.888	4260.692	1624.236	4399.577
5	1031.938	4836.545	1235.089	5281.803	1512.267	5772.959	1719.815	6119.393
6	899.024	5735.569	1187.263	6469.066	1415.888	7188.847	1735.819	7855.212
7	653.385	6388.954	1032.839	7501.905	1387.328	8576.176	1558.497	9413.709
8	-		1224.816	8726.721	1290.984	9867.160	1551.441	10965.150
9			-		1200.903	11068.063	1417.535	12382.685
10					1098.099	12166.162	1467.200	13849.885
11					824.505	12990.667	1332.484	15182.369
12					-		1281.131	16463.500
13							1121.861	17585.361
14							1316.555	18901.916

Table 15. Comparison of max energy dissipation for 28 MPa and 55 MPa

Sample	Max Energy dissipated (kN.mm)	% Increase in energy	Sample	Max Energy dissipated (kN.mm)	% Increase in energy
4K0MM	6182	-	8K0MM	6388	-
4K2MM	9141	47.9	8K2MM	8726	36.6
4K4MM	12912	108.9	8K4MM	12990	103.4
4K6MM	18919	206.0	8K6MM	18901	195.9

CHAPTER 6

CONCLUSIONS AND RECOMMENDATIONS

Based on the parameters and variables studied in this study for both; normal strength reinforced concrete columns and high strength reinforced concrete columns, the following conclusions are made:

6.1 Conclusions

1 The overall performance of RC columns was also enhanced with a plodding failure mechanism and increase in overall load bearing capacity.

2 The capacity for loads and displacement at peak and ultimate points increased up to 68.98%, 54.28%, 82.58% and 75.40%, respectively, for 28 MPa concrete columns.

3 Confinement effects the load bearing capacity more than the load bearing capacity.

4 The effect on high strength concrete is more for displacements than load bearing capacity.

5 The ductility index increased to a maximum value of 12.4% for 28 Mpa and 16.4% for 55 MPa.

6 The effect of confinement on ductility is more for high strength concrete than the normal strength concrete columns.

7 The energy dissipation capacity is improved by approximately 200% for high strength RC columns and more than 200% for normal strength RC columns.

8 It is noted that the amount of energy dissipated in each consecutive cycle increases till peak point and decreases after the peak point till the failure occurs.

9 Most of energy is dissipated when the columns undergo significant plastic deformations.

6.2 Recommendations

As it is evident from the results that Polyurea is very effective to be used as a confinement technique, it is suggested that the proposed confinement technique can be used for real-time engineering projects.

Following recommendations are suggested for future research projects:

1 This study was based on Finite Element Method. It needs to be validated through experimental study.

2 Constitutive model for RC Columns confined with Polyurea can be developed.

3 The effectiveness of confinement is studied only for cyclic axial compressive loads. It can be further extended to combined axial and lateral loadings.

4 From literature it is studied that Polyurea increase the shear and flexural capacity of small scale and large scale beams. Polyurea can be investigated for partial replacement on transverse reinforcement, particularly in the regions having a higher volume of transverse reinforcement.

REFERENCES

1. A. E. Marawan, A. S. Debaiky and N. N. khalil. "Shear and flexural behaviour of RC beams strengthened with ployurea spray." 2015. IJARSE, ISSN 2319-8354, Vol 4, Issue 11, pg (12-26).
2. A. Kelsey, John H. "Energy theorems and structural analysis." 1960. Springer.
3. A. V. Amirkhizi, J. Isaacs , J. McGee & S. Nemat-Nasser. "An experimentally-based viscoelastic constitutive model for Polyurea, including pressure and temperature effects." 2006. Philosophical Magazine, Volume 86 - Issue 36, pp. 5847-5866.
4. A., Shafqat A. and Ali. "Lateral confinenment of RC short columns." 2012 . Sci.Int.(Lahore), 24(4), 371-379.
5. Ahmed M. El-Kholy, Hany A. Dahish b. "Improved confinement of reinforced concrete columns." 2016. Ain Shams Engineering Journal Vol: 7, 717–728.
6. Ahmeda, C.Ali, and K. Ait Tahara. "Behavior of concrete cylinder confined with helical composites." 2015. Procedia Engineering, Vol: 114, Page: 157-164.
7. Ali Khajeh Samani, Mario M. Attard. "A stress–strain model for uniaxial and confined concrete under compression." 2012. Engineering Structures 41, 335–349.
8. Amir Mirmiran, Mohsin Shahaway. "Behavior of Concrete Columns Confined by Fiber Composites." 1997. Journal of Structural Engineering, Vol: 123, Issue:5 .
9. Argyris, J. H. "Energy theorems and structural analysis." 1954. Aircraft Engineering and Aerospace Technology.
10. B. Doran, H. Koksal, and T. Turgay. "Nonlinear finite element modeling of rectangular/square concrete columns confined with FRP." 2009. Materials & Design, vol.30, no. 8, pp. 3066-3075.

11. BASF. "Technical documentation made available by BASF Polska."

12. Bathe, K.-J. "Frontiers in finite element procedures & applications." 2014. Computational Methods for Engineering Science.

13. C. C. Weng, Y. L. Yin, J. C. Wang, C. H. Shih. "Axial strength and ductility of rectangular SRC columns with innovative double spiral confinement." October 12-17, 2008, Beijing, China. The 14th World Conference on Earthquake Engineering.

14. C. S. Lewangamage, C. K. Rankoth and M. T. R. Jayasinghe. "A Study on Reinforced Concrete Columns Partially Confined with Carbon Fibre Reinforced Polymers." 2017. Engineer, Vol. L, No. 04, pp. [41-50].

15. C.Gamonpilas, R.McCuiston. "A non-linear viscoelastic material constitutive model for Polyurea." 2012. Polymer, Volume 53, Issue 17, Pages 3655-3658.

16. Chee Loong Chin, Ma Chau Khun, Tan Jia Yang, Abdullah Zawawi Awang. "Effect Of Pre-Tensioned Level on Axial Stress-Strain Behaviour of Confined Concrete: A Review." 2018. International Journal of Engineering & Technology 7(3.9).

17. Chul Min Cho, Ji Hun Choi, Seung Hoon Rhee, Tae Kyun Kim, Jang Ho Jay Kim. "Material Performance Evaluation of Polyurea for Structural Seismic Retrofitting." 2017. Journal of the Korea Concrete Institute Vol. 29, No. 2, 131-139.

18. Chunya Li, Jim Lua. "A hyper-viscoelastic constitutive model for Polyurea." 2009. Materials Letters, Volume 63, Issue 11, Pages 877-880.

19. Courant, R. "Variational methods for the solution of problems of equilibrium and." 1943. Verlag nicht ermittelbar.

20. Dahl, Kaare K. B. "A Constitutive Model for Normal and High Strength Concrete." 1992. Technical University of Denmark, Department of Civil Engineering.

21. Damith Mohotti, Muneeb Ali, Tuan Ngo, Jinghan Lu, Priyan Mendis. "Strain rate dependent constitutive model for predicting the material behaviour of Polyurea under high strain rate tensile loading." 2014. Materials and Design 53, 830–837.

22. E., Hognestad. "Study of combined bending and axial load in reinforced concrete." 1951.

23. Endah Safitri, Iswandi Imran and Nuroji. "Concrete Strength ehancement due to external steel ring confinement." 2017 . Procedia Engineering 171, 934 – 939 .

24. Frank E. Ritchart, Anton Brandtzaeg, Rex L. Brown. "A study of the failure of concrete under combined compressive stresses." 1928. University of Illinois, Engineering experiment station, Vol: 26(12) Page:1-92.

25. G. Campione, L. Cavaleri, F. Di Trapani. "Frictional effects in structural behavior of no-end-connected steel-jacketed RC columns." 2017. Journal of Structural Engineering, vol. 143, no. 8, pp. 04017070.

26. Grujicic M, He T, Pandurangan B, Svingala FR, Settles GS, Hargather MJ. "Experimental characterization and material-model development for microphase-segregated Polyurea: an overview." 2012. J Mater Eng Perform;21(1):2–16.

27. Hao Wang, Ximin Deng, Haijun Wu, Aiguo Pi, Jinzhu Li, Fenglei Huang. "Investigating the dynamic mechanical behaviors of Polyurea through experimentation and modeling." 2019. Defence Technology, Volume 15, Issue 6, Pages 875-884.

28. Hasan Moghaddam, Maysam Samadi, Kypros Pilakoutas. "Axial compressive behavior of concrete actively confined by metal strips; part A: experimental study." 2010. Materials and Structures - 43: 1369.

29. Hollomon, J. H. "Tensile deformation." 1945. Transaction of American Institute of Mechanical Engineering, vol. 162, pp. 268–277.

30. Hugo. Rodrigues, Humberto. Varum, António. Arêde, Aníbal. Costa. "A comparative analysis of energy dissipation and equivalent viscous damping of RC columns subjected to uniaxial and biaxial loading." 2012. Engineering Structures 35 (149–164).

31. J. B. Mander, M.J.N. Priestly and R. Park. "Theoritical stress strain model for confined concrete." 1988. J. Struct. Eng., 114(8): 1804-1826 .

32. J. Szafran, A. Matusiak. "Polyurea coating systems: Definition, reseearch and applications." 2016. LIGHTWEIGHT STRUCTURES in CIVIL ENGINEERING, XXII LSCE.

33. Jacek Szafran, Artur Matusiak. "Crushing strength of concrete rings with a Polyurea reinforce system." 2020. Tunnelling and Underground Space Technology,Volume 101, 103407.

34. James S. Davidson, Jonathan R. Porter, Robert J. Dinan, Michael I. Hammons, James D. Connell. "Explosive Testing of Polymer Retrofit Masonry Walls." 2004. J. Perform. Constr. Facil.18:100-106.

35. Kent D, Park R. " Flexural members with confined concrete." 1971. ASCEJ Struct Div; 97:1964–1990.

36. Khan, Mohiuddin Ali. *Earthquake resistant structures.* Butterworth: Heinemann, Pages 283-315, 2013.

37. L.-H. Han, F.-Y. Liao, Z. Tao. "“Performance of concrete filled steel tube reinforced concrete columns subjected to cyclic bending." 2009. Journal of Constructional Steel Research, vol. 65, no. 8-9, pp. 1607-1616.

38. Li, K. S. Zhano and Z. H. "Numerical analysis of the stress-strain curve and fracture initiation for ductile material." 1994. Engineering Fracture Mechanics, vol. 49, no. 2, pp. 235–241.

39. Ling, Y. "Uniaxial true stress-strain after necking." 1996. AMP Journal of Technology, vol. 5, pp. 37–48.

40. Liu, Y., Y. Liao, N. Zheng, and J. Liu. *Analysis of Strong Column and Weak Beam Behavior of Steel-concrete Mixed Frames. In The 15th World Conference on Earthquake Engineering, Lisboa.* In The 15th World Conference on Earthquake Engineering, Lisboa., 2012.

41. M. Bruneau, C. M. Uang, and A. Whittaker. "Ductile Design of Steel Structures." 1998. McGraw-Hill, New York, NY, USA.

42. M. J. Turner, R. W. Clough, H. C. Martin. "Stiffness and deflection analysis of complex structures." 1956. journal of the Aeronautical Sciences, vol. 23, no. 9, pp. 805-823.

43. M. Maj, A. Ubysz. "Polyurea insulations as insulating material with multilateral use (in Polish)." 2017. Civil Engineer, 6, pp. 75-81.

44. M. Rizwan, M. Chaudhary, M. Ilyas. "Computer based estimation of backbone curves for hysteretic Response of reinforced concrete columns under static cyclic lateral loads." 2014. Computers and Concrete, vol. 14, no. 2, pp. 193-209.

45. M. Rizwan, S. A. Khan, M. Ilyas. "Modelling steel-strip-confined reinforced concrete columns." 2016. Proceedings of the Institution of Civil Engineers-Structures and Buildings, vol. 169, no. 4, pp. 245-256.

46. M., Sargin. "Stress–strain relationships for concrete and the analysis of structural concrete sections." 1971. Solid mechanics division. University of Waterloo.

47. Mahmoud F.Belal, Hatem M.Mohamed, Sherif A.Morad. "Behavior of reinforced concrete columns strengthened by steel jacket." 2015. HBRC Journal, Volume 11, Issue 2, Pages 201-212.

48. Mander, J. B., M. J. N. Priestley, and R. Park. "Theoretical stress strain model of confined concrete." *Journal of Sructural Engineering*, 1988: 114(8), 1804-1826.

49. Minafò, G. "Analytical modelling of force transmission in axially loaded RC columns with indirectly loaded jackets." 2019. Engineering Structures, vol. 181, pp. 15-26.

50. Murat. Saatcioglu, Salim. R. Razvi. "STRENGTH AND DUCTILITY OF CONFINED CONCRETE." *Journal of Structural engineering, 118(6), 1590-1607.*, 1992.

51. Naveed, Anwar, and Ahmed, Najam Fawad. *Structural Cross Sections, Analysis and Design,Pages 391-481.* Butterworth: Heinemann, 2017.

52. Ndubuaku Onyekachi, Martens Michael, Ahmed Arman, Cheng Roger, Adeeb Samer. "A novel approach for stress strain characterization of metallic materials using the product log(Omega) function." 2017. Leadership in Sustainable Infrastructure.

53. Nomesh Kumar, V. Venkateswara Rao. "Hyperelastic Mooney-Rivlin Model: Determination and Physical Interpretation of Material Constants." 2016. MIT International Journal of Mechanical Engineering, Vol. 6, No. 1, pp. 43-46.

54. O. C. Zienkiewicz, and Y. K. Cheung. "The finite element method for analysis of elastic isotropic and orthotropic slabs." 1964. Proceedings of the Institution of Civil Engineers, vol. 28, no. 4, pp. 471-488.

55. P. Arasaratnam, K. S. Sivakumaran and M. J. Tait. "True Stress-True Strain Models for Structural Steel Elements." 2011. International Scholarly Research Notices.

56. Popovics, Sandor. "A numerical approach to complete stress strain curve of concrete." 1973. CEMENT and CONCRETE RESEARCH. Vol. 3, pp. 583-599.

57. R. Basset, S. M. Uzumeri. "Effect of confinement on the behaviour of high-strength lightweight concrete columns." 2011. Canadian Journal of Civil Engineering 13(6):741-751 · .

58. R. W. Clough, and C. P. Johnson. "“A finite element approximation for the analysis of thin shells." 1968. International Journal of Solids and Structures, vol. 4, no. 1, pp. 43-60.

59. Rami Eid, Patrick Paultre. "Compressive behavior of FRP-confined reinforced concrete columns." *Engineering Structures 132*, 2017: 518–530.

60. Riad Babba, Abdelghani Merdas. "Width Effect of CFRP Strips on the Compressive Behavior of Plain Concrete Cylinders." 2020. Iranian Journal of Science and Technology, Transactions of Civil Engineering volume 44, pages921–929.

61. S. N. Raman, M. Jamil, T. Ngo, P. Mendis & T. Pham. "Retrofitting of RC panels subjected to blast effects using elastomeric polyumer coatings." 2014. Proceedings of Concrete Solutions, 5th International Conference on Concrete Repair, At Belfast, UK.

62. Sargin M, Ghosh S, Handa V. "Effects of lateral reinforcement upon the strength and deformation properties of concrete." 1971. Mag Concr Res; 23:99–110.

63. Sarva SS, Deschanel S, Boyce MC, Chen W. "Stress-strain behavior of Polyurea and a polyurethane from low to high strain rates." 2007. Polymers: 48(8) pp. 2208-2213.

64. Shanaka. Kristombu. Baduge, Priyan. Mendis, Tuan. Duc. Ngo & Massoud. Sofi. "Ductility Design of Reinforced Very-High Strength Concrete Columns ." 2019. Int J Concr Struct Mate 13:37.

65. Synge, J. L. "Orbits and rays in the gravitational field of a finite sphere according to the theory of AN Whitehead." 1952. Proceedings of the Royal Society of London. Series A. Mathematical and Physical Sciences, vol. 211, no. 1106, pp. 303-319.

66. T. Tavio, I. Wimbadi, A. K. Negara. "Effects of confinement on interaction diagrams of square reinforced concrete columns." 2009. Civil Engineering Dimension, vol.11, no. 2, pp. 78-88.

67. T. Yu, J. Teng, Y. Wong. "“Finite element modeling of confined concrete-II: Plastic-damage model." 2010. Engineering structures, vol. 32, no. 3, pp. 680-691.

68. Theodoros C. Rousakis, Ioannis S. Tourtouras. "RC columns of square section – Passive and active confinement with composite ropes." 2014. Composites: Part B 58, 573–581.

69. Wang P, Shah S, Naaman A. " Stress–strain curves of normal and lightweight concrete in compression. ." 1978. ACI.

70. WELSIM. "Mooney-Rivlin hyperelastic model for nonlinear finite element analysis." Finite Element Analysis Solutions.

71. YE, L. P., Q. L. MA, and Z. W. MIAO. "Study on weak beam-strong column design method of RC frame structures." *Engineering Mechanics, 12.* (Engineering Mechanics, 12.), 2010.

72. Yi J., Boyce MC, Lee GF, Balizer E. " Large deformation rate dependent stress-strain behavior of Polyurea and polyurethanes." 2006. Polymer: 47(1) pp. 319-329.